

CHAPTER 10 PROBLEMS AND EXERCISES

Problem 1: Consider a steel beam of thickness $h_1 = 2.6$ mm, width $b_1 = 8$ mm, length $l = 100$ mm, and material properties given in Table 10.1. A 7-mm square PWAS ($l_a = 7$ mm, $b_a = 7$ mm, $t_a = 0.22$ mm) is bonded to the beam surface at $x_a = 40$ mm from the left hand end. The material properties of the PWAS are given in Table 10.2. Assume 1% mechanical damping and electric loss. (i) Use the 1-D analytical expressions deduced in this chapter to calculate the admittance and impedance response in the interval 1 kHz to 30 kHz of the PWAS attached to the structure. (ii) Plot superposed on the same chart (with appropriate scale factors) the admittance and impedance real parts and the frequency response function imaginary part. Comment on the significance of the peaks observed in these plots.

Solution

Note: the structural damping is not given; we take it $\zeta = 0.5\%$

(i) To calculate the admittance and impedance response of the PWAS as attached to the structure, use the constraint PWAS expressions given in textbook Eqs. (10.3) and (10.4), i.e.,

$$Y = i\omega \bar{C} \left[1 - \bar{k}_{31}^2 \left(1 - \frac{1}{\bar{\varphi} \cot \bar{\varphi} + \bar{r}} \right) \right] \quad (\text{constraint PWAS admittance}) \quad (10.3) \quad (1)$$

$$Z = \frac{1}{i\omega \bar{C}} \left[1 - \bar{k}_{31}^2 \left(1 - \frac{1}{\bar{\varphi} \cot \bar{\varphi} + \bar{r}} \right) \right]^{-1} \quad (\text{constraint PWAS impedance}) \quad (10.4) \quad (2)$$

where $\bar{\varphi} = \frac{1}{2} l_a \bar{\gamma}_{PWAS}$, γ is the wave number $\bar{\gamma}_{PWAS} = \omega/c_{PWAS}$ and \bar{r} is the stiffness ratio. Note that $\bar{\varphi}$, $\bar{\gamma}_{PWAS}$, \bar{r} are complex-number functions of ω . The stiffness ratio, \bar{r} , is calculated with textbook Eq. (10.7), i.e.,

$$\bar{r}(\omega) = \frac{\bar{k}_{str}(\omega)}{\bar{k}_{PWAS}}, \quad (10.7) \quad (3)$$

where $\bar{k}_{str}(\omega)$ is the frequency-dependent structural dynamic stiffness and \bar{k}_{PWAS} is the PWAS static stiffness given by textbook Eq. (10.8), i.e.,

$$\bar{k}_{PWAS} = \frac{b_a t_a}{\bar{s}_{11}^E l_a} \quad (10.8) \quad (4)$$

The complex-number expressions of material properties are obtained by using the PWAS mechanical damping and electrical loss factors η, δ as shown in Eqs. (9.99), (9.101), i.e.,

$$\bar{s}_{11}^E = s_{11}^E (1 - i\eta), \quad \bar{\varepsilon}_{33}^T = \varepsilon_{33}^T (1 - i\delta) \quad (9.99) \quad (5)$$

$$\bar{k}_{13}^2 = \frac{d_{31}^2}{\bar{s}_{11}^E \bar{\varepsilon}_{33}^T}, \quad \bar{C} = \bar{\varepsilon}_{33}^T \frac{b_a l_a}{t_a}, \quad \bar{c} = \sqrt{\frac{1}{\rho_a \bar{s}_{11}^E}}, \quad \bar{\varphi} = \frac{1}{2} \frac{\omega l_a}{\bar{c}} \quad (9.101) \quad (6)$$

The frequency-dependent structural dynamic stiffness, $k_{str}(\omega)$, is calculated by performing the dynamic analysis of the steel beam undergoing forced vibration under PWAS excitation. This analysis, which is an extension of the conventional beam vibration analysis is presented in detail

in textbook Section 10.2.2, and will not be repeated here. Essentially, one arrives at the dynamic stiffness expression given by the textbook Eq. (10.41), i.e.,

$$\bar{k}_{str}(\omega) = \frac{\hat{F}_{PWAS}}{\hat{u}_{PWAS}} = \rho A \left\{ \sum_{j_u=N_u^{low}}^{N_u^{high}} \frac{\left[U_{j_u}(x_a + l_a) - U_{j_u}(x_a) \right]^2}{\omega_{j_u}^2 + 2i\zeta_{j_u}\omega_{j_u}\omega - \omega^2} + \left(\frac{h}{2} \right)^2 \sum_{j_w=N_w^{low}}^{N_w^{high}} \frac{\left[W'_{j_w}(x_a + l_a) - W'_{j_w}(x_a) \right]^2}{\omega_{j_w}^2 + 2i\zeta_{j_w}\omega_{j_w}\omega - \omega^2} \right\}^{-1} \quad (10.41) (7)$$

Equation (7) involves the use of the axial and flexural vibration modeshapes, $U_{j_u}(x)$ and $W_{j_w}(x)$, where j_u and j_w are mode indices that span the frequency band of interest. For free-free beams, the axial and flexural mode shapes can be calculated with the formulae (10.14), (10.23), (10.24), i.e.,

$$U_{j_u}(x) = \sqrt{\frac{2}{l}} \cos \gamma_{j_u} x, \quad \gamma_{j_u} = j_u \frac{\pi}{l}, \quad \omega_{j_u} = j_u \frac{\pi}{l} \sqrt{\frac{E}{\rho}}, \quad j_u = N_u^{low} \dots N_u^{high} \quad (10.14) (8)$$

$$W_{j_w}(x) = \frac{1}{\sqrt{l}} \left[(\cosh \gamma_{j_w} x + \cos \gamma_{j_w} x) - \beta_{j_w} (\sinh \gamma_{j_w} x + \sin \gamma_{j_w} x) \right] \quad (10.23) (9)$$

$$\gamma_{j_w} = \frac{z_{j_w}}{l}, \quad \omega_{j_w} = \gamma_{j_w}^2 \sqrt{\frac{EI}{\rho A}}, \quad j_w = N_w^{low} \dots N_w^{high} \quad (10.24) (10)$$

with the eigenvalues z_j and the modeshape factors β_j being given in Chapter 3. The eigenvalues z_j are obtained as the solution of the transcendental equation Eq. (3.406), i.e.,

$$\cos z \cosh z - 1 = 0 \quad (3.406) (11)$$

The modeshape factors are calculated with Eq. (3.411), i.e.,

$$\beta_{j_w} = \frac{\cosh \gamma_{j_w} l - \cos \gamma_{j_w} l}{\sinh \gamma_{j_w} l - \sin \gamma_{j_w} l} = \frac{\sinh \gamma_{j_w} l + \sin \gamma_{j_w} l}{\cosh \gamma_{j_w} l - \cos \gamma_{j_w} l} \quad (3.411)(12)$$

In actual practice it is advisable to use the numerically stable formulation Eq. (3.431) instead of Eq. (9), i.e.,

$$W_j(x) = A_j \left[\cos \gamma_j x - \beta_j \sin \gamma_j x + \frac{1}{2} (1 - \beta_j) e^{\gamma_j x} + \frac{1}{2} (1 + \beta_j) e^{-\gamma_j x} \right] \quad (3.431)(13)$$

where $j = j_w$. The mode slopes W'_j are calculated through the differentiation of Eq. (13), i.e.,

$$W'_j(x) = A_j \gamma_j \left[-\sin \gamma_j x - \beta_j \cos \gamma_j x + \frac{1}{2} (1 - \beta_j) e^{\gamma_j x} - \frac{1}{2} (1 + \beta_j) e^{-\gamma_j x} \right] \quad (14)$$

For the numerical values given in this problem, one obtains the following natural frequencies:

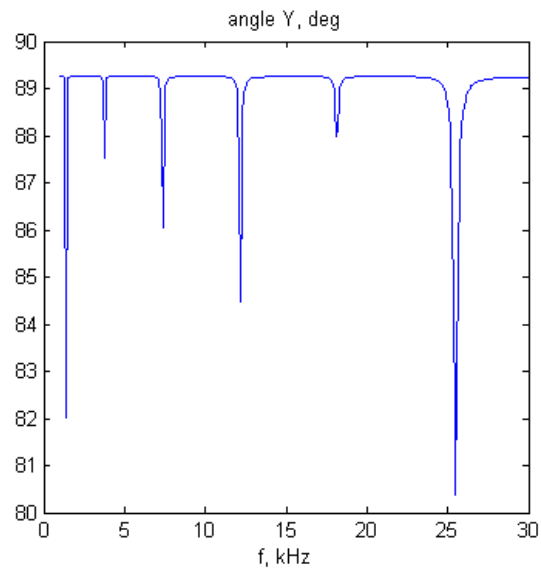
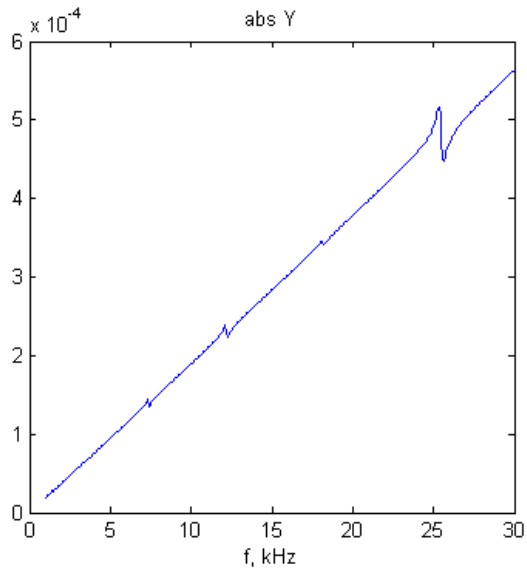
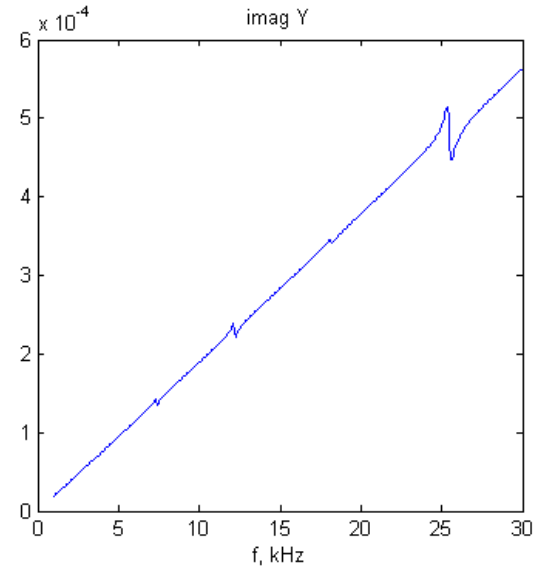
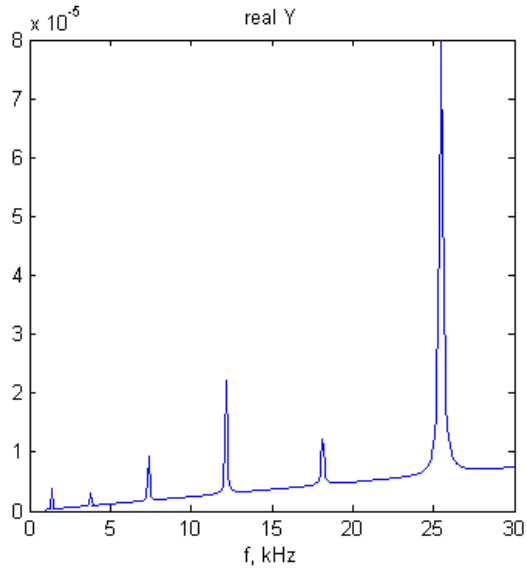
Axial frequencies: $f_{j_u} = 25.4, 50.8 \text{ kHz}$, $j_u = 1, 2$

Flexural frequencies: $f_{j_w} = 1.358, 3.74, 7.34, 12.13, 18.12, 25.3 \text{ kHz}$, $j_w = 1, \dots, 6$

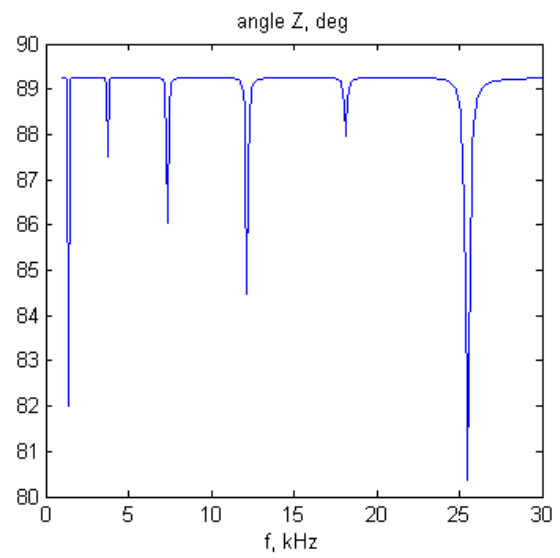
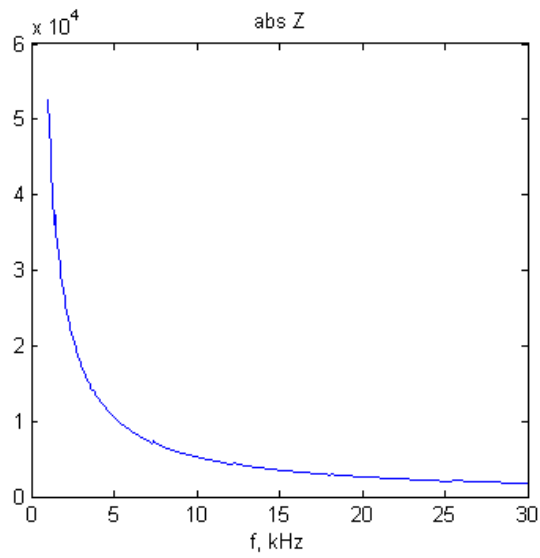
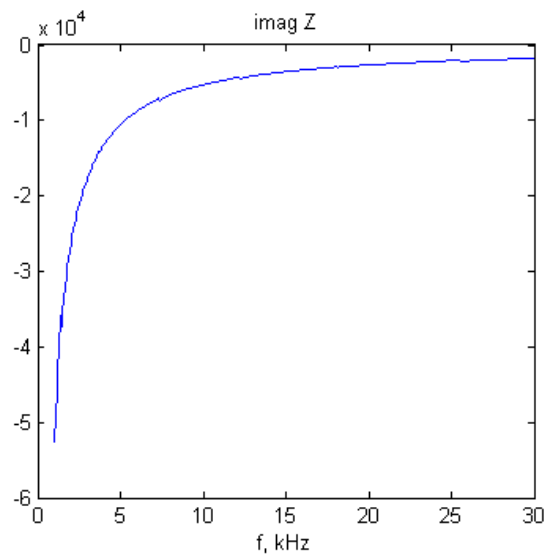
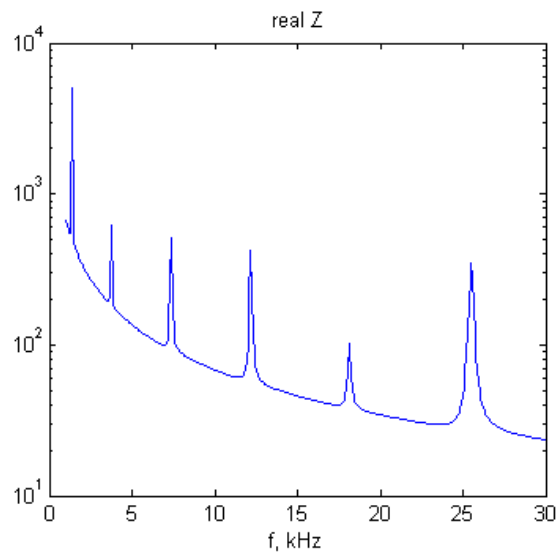
It should be noted that the first axial frequency and the sixth flexural frequencies are very close, i.e., $f_1^u = f_{1_u} = 25.4 \text{ kHz}$, $f_6^w = f_{6_w} = 25.3 \text{ kHz}$. This fact may produce overlap in the plots.

The admittance and impedance plots are as follows:

Admittance:



Impedance:

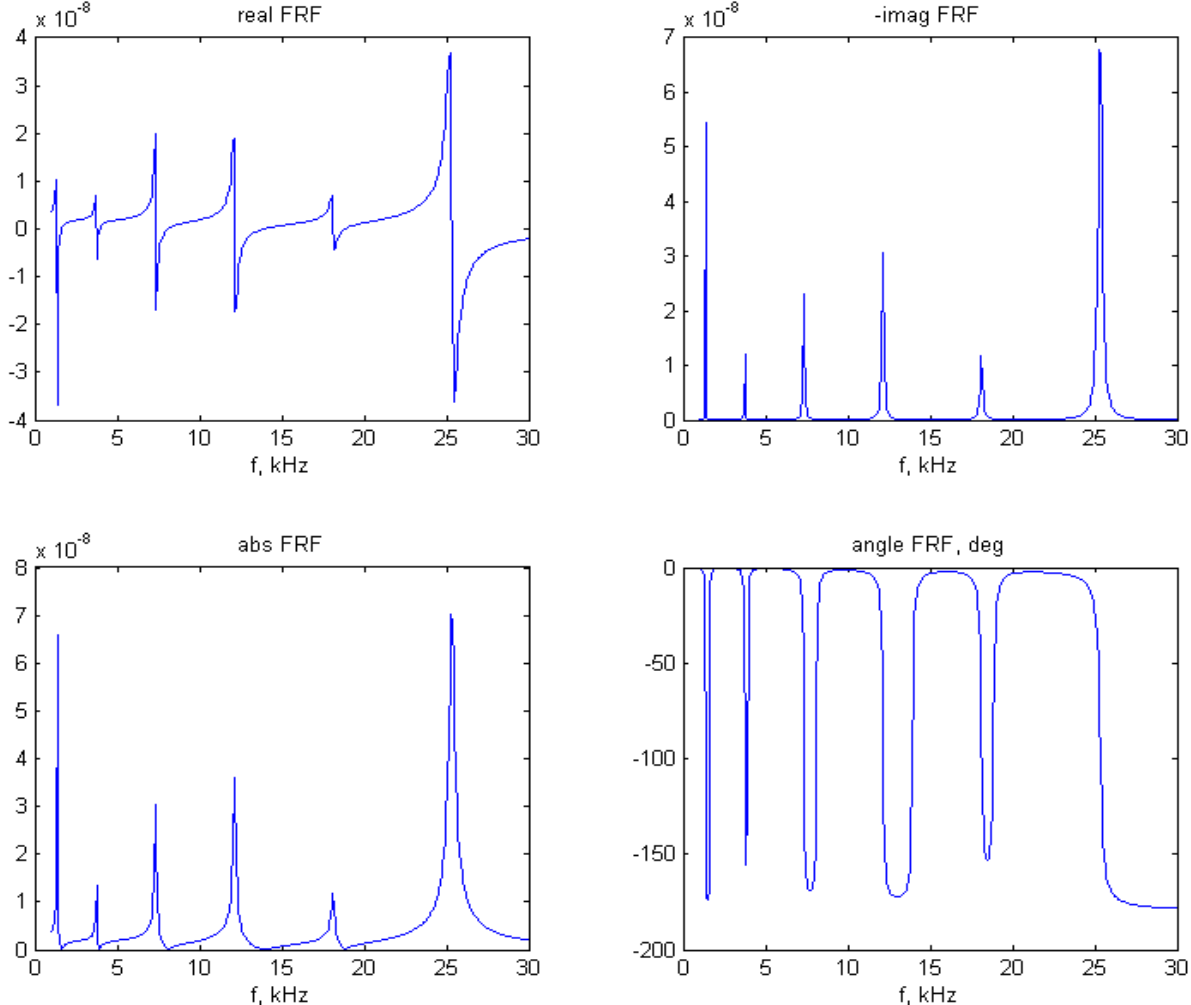


=====

(ii) The frequency response function is calculated with the textbook Eq. (10.36), i.e.,

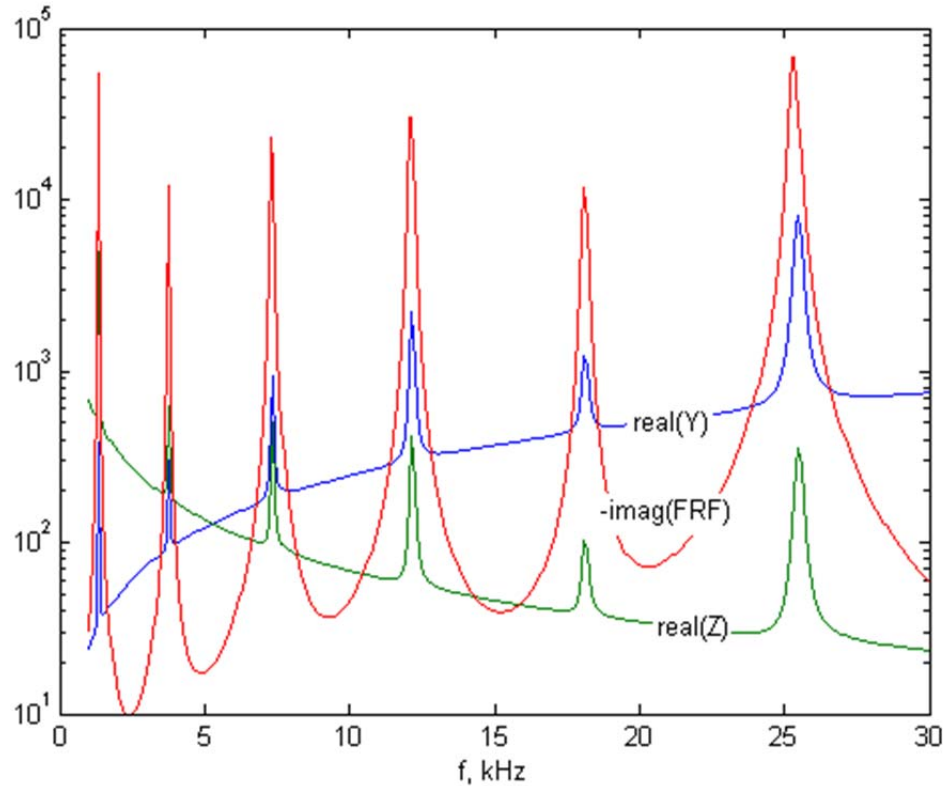
$$FRF(\omega) = \frac{\hat{u}_{PWAS}}{\hat{F}_{PWAS}} = \frac{1}{\rho A} \left\{ \sum_{j_u} \frac{[U_{j_u}(x_a + l_a) - U_{j_u}(x_a)]^2}{\omega_{j_u}^2 + 2i\zeta_{j_u}\omega_{j_u}\omega - \omega^2} + \left(\frac{h}{2}\right)^2 \sum_{j_w} \frac{[W'_{j_w}(x_a + l_a) - W'_{j_w}(x_a)]^2}{\omega_{j_w}^2 + 2i\zeta_{j_w}\omega_{j_w}\omega - \omega^2} \right\} \quad (10.36)(15)$$

One notes that Eq. (15) giving the frequency response function (FRF) is the inverse of Eq. (7) giving the dynamic stiffness matrix. The FRF plot is given below.



As discussed earlier in Chapter 3, which deals with vibration analysis, the peaks of the FRF imaginary part correspond to resonance frequencies. In the frequency band of interest (1-30 kHz) there are six structural resonances ($f_1 = 1.36$ kHz, $f_2 = 3.74$ kHz, $f_3 = 7.34$ kHz, $f_4 = 12.13$ kHz, $f_5 = 18.12$ kHz, $f_6 = 25.4$ kHz). The first five resonances are due to flexural vibration, whereas the sixth is due to an overlap of the first axial resonance ($f_1^u = 25.4$ kHz) and the sixth flexural resonance ($f_6^w = 25.3$ kHz).

The superposed plots (with appropriate scale factors) of the admittance and impedance real parts and the frequency response function imaginary part are given next.



One observes that the peaks of the three curves represented in these plots align perfectly. This indicates that the admittance and impedance real parts follow with fidelity the structural resonances $f_1 = 1.36 \text{ kHz}$, $f_2 = 3.74 \text{ kHz}$, $f_3 = 7.34 \text{ kHz}$, $f_4 = 12.13 \text{ kHz}$, $f_5 = 18.12 \text{ kHz}$, $f_6 = 25.4 \text{ kHz}$ as depicted by the structural frequency response function $-\text{imag}(\text{FRF})$ at the PWAS location.

```

1 % Ch.10 Problems 10.1, 10.2 (steel beams)
2 % Copyright Victor Giurgiutiu: SHM with PWAS book
3 clc
4 clear
5 %% DEFINE PROPERTIES
6 mm=1e-3; L=100*mm; b0=8*mm; h0=2.6*mm; E=200e9; p=7750; % steel beam
7 b=b0; h=h0; % Problem 10.1 and Problem 10.2 Case 1
8 % b=b0; h=2*h0; % Problem 10.2 Case 2 narrow thick beam
9 % b=19.6*mm; h=h0; % Problem 10.2 Case 3 wide thin beam
10 % b=19.6*mm; h=2*h0; % Problem 10.2 Case 4 wide thick beam
11 I=(b*h^3)/12; A=b*h; % cross section properties
12 zeta=5e-3; % structural damping
13 La=7e-3; ba=7e-3; ta=0.22e-3; % PWAS geometry
14 sE11=15.30e-12; e0=8.85e-12; eT33=1750*e0; d31=-175e-12; pa=7700; % PWAS material
15 xA=40e-3; xB=xA+La; % PWAS location on steel beam
16 %% DEFINE FREQUENCY RANGE
17 kHz=1e3; % shorthand for kHz
18 Nf=401; % number of frequencies in the spectrum
19 fStart=1*kHz; % start frequency
20 fEnd=30*kHz; % end frequency
21 df=(fEnd-fStart)/(Nf-1); % frequency increment
22 f=fStart:df:fEnd; w=2*pi*f; % frequency range, f in Hz; w in rad/s
23 %% CALCULATE NATURAL FREQUENCIES AND MODESHAPES
24 Nx=1e3; dx=L/(Nx-1); x=0:dx:L; % discretize beam length
25 %% Axial frequencies and modeshapes: Eq. (10.14)
26 ffU=0; jU=0; NU_low=0; % starting values for the iteration loop
27 while ffU<=fEnd % identify the required number of axial modes
28     jU=jU+1;
29     wU(jU)=jU*pi*sqrt(E/p)/L; % store axial angular frequencies in rad/s
30     fU(jU)=wU(jU)/(2*pi); % store axial frequency in Hz
31     ffU=wU(jU)/(2*pi); % local value of frequency for the iteration loop
32     NU_low=NU_low+1*(ffU<fStart); % increment lower limit of mode index range
33 % Calculate modeshapes: Eqs. (10.14)
34 gU=jU*pi/L;
35 U(:,jU)=sqrt(2/L)*cos(gU*x); % axial modeshapes Eq. (10.14)
36 U_xA=sqrt(2/L)*cos(gU*xA); U_xB=sqrt(2/L)*cos(gU*xB);...
37     dU(jU)=U_xB-U_xA; % axial displacement diff at PWAS edges xA, xB
38 end
39 NU_low=1*(NU_low<1)+NU_low*(NU_low>=1); % lower limit on the axial modes index
40 NU_high=jU; % number of required axial modes
41 display([jU,fU/kHz], 'jU, fU, kHz') % axial frequencies
42 display([fStart/kHz fEnd/kHz], 'fStart fEnd, kHz') % frequency range
43 display([NU_low, NU_high], 'NU_low, NU_high') % axial mode index range
44
45 figure(1); plot(x,U);grid; title ('Axial modes')
46 %% Flexural frequencies and modeshapes
47 % calculate flexural eigenvalues: solve Eq. (3.406)
48 % Calculate flexural frequencies
49 funcW=@(z)(cos(z)-1/cosh(z)); % characteristic eq. for free-free flexural vibr.
50 % f=@(x)(cos(x)*cosh(x)-1); this equation is less accurate - do not use
51 ffW=0; jW=0; NW_low=0; % starting values for the iteration loop

```

```

52 j=1:1:20; zWg(j)=(2*j+1)*pi/2; % initial guess for flexural eigenvalues
53 while ffW<=fEnd % identified the required number of flexural modes
54     jW=jW+1;
55     z=fzero(funcW,zWg(jW)); % solve flex. transcendal eq.
56     zW(jW)=z; % flexural eigenvalues
57     gW=z/L; % flexural eigenvalues
58     wW(jW)=gW^2*sqrt(E*I/(p*A)); % flexural angular frequency in rad/s
59     fW(jW)=wW(jW)/(2*pi); % store flexural frequency in Hz
60     ffW=fW(jW); % local value of flexural frequency for the interation loop
61 % Calculate modeshapes: Eqs. (3.411), (10.23), (3.431)
62     beta=(sinh(z)+sin(z))/(cosh(z)-cos(z));
63     W(:,jW)=1/sqrt(L)*((cos(gW*x)-beta*sin(gW*x)...
64         +(1-beta)/2*exp(gW*x)+(1+beta)/2*exp(-gW*x))); % Eq. (10.23)
65     W1_xA=1/sqrt(L)*gW*((-sin(gW*xA)-beta*cos(gW*xA)...
66         +(1-beta)/2*exp(gW*xA)-(1+beta)/2*exp(-gW*xA)));
67     W1_xB=1/sqrt(L)*gW*((-sin(gW*xB)-beta*cos(gW*xB)...
68         +(1-beta)/2*exp(gW*xB)-(1+beta)/2*exp(-gW*xB)));
69     dW1(jW)=W1_xB-W1_xA; % flex slopes diff at PWAS edges xA, xB
70 end
71
72 NW_low=1*(NW_low<1)+NW_low*(NW_low>=1); % lower limit on the flex modes index
73 NW_high=jW; % upper limit on the flexural modes index
74 % display(zW,'zW') % flexural eigenvalues
75 display([jW,fW/kHz], 'jW, kHz') % flexural frequencies
76 display([fStart/kHz fEnd/kHz], 'fStart fEnd, kHz') % frequency range
77 display([NW_low, NW_high], 'NW_low, NW_high') % flexural mode index range
78
79 figure(2); plot(x,W); grid; title('Flexural modes')
80 % =====
81 %% START FREQUENCY LOOP TO CALCULATE FREQUENCY RESPONSE FUNCTIONS
82 ff=f/kHz; % freq in kHz for plotting
83 %% AXIAL RESPONSE
84 for nf=1:Nf % frequency loop
85     ww=w(nf);
86     % axial modes loop
87     sum_U=0;
88     for jU=NU_low:1:NU_high
89         num=(p*A)*dU(jU)^2; den=(wU(jU)^2+2*li*zeta*wU(jU)*ww-ww^2);
90         sum_U=sum_U+num/den;
91     end
92     FRF_U(nf)=sum_U;
93 end
94 %% PLOT AXIAL FRF
95 figure(3) % FRF_U plots
96 subplot(2,2,1); plot(ff,real(FRF_U));title('real FRF_U'); xlabel('f, kHz')
97 subplot(2,2,2); plot(ff,-imag(FRF_U));title('-imag FRF_U'); xlabel('f, kHz')
98 subplot(2,2,3); plot(ff,abs(FRF_U)); title('abs FRF_U'); xlabel('f, kHz')
99 %     set(gca,'Yscale','log');
100 subplot(2,2,4); plot(ff,180/pi*angle(FRF_U));...
101     title('angle FRF_U, deg'); xlabel('f, kHz')
102 %% FLEXURAL RESPONSE

```

```

103 for nf=1:Nf % frequency loop
104   ww=w(nf);
105   % flexural modes loop
106   sum_Wl=0;
107   for jW=NW_low:1:NW_high
108     num=(h/2)^2/(p*A)*dWl(jW)^2; den=(ww(jW)^2+2*li*zeta*wW(jW)*ww-ww^2);
109     sum_Wl=sum_Wl+num/den;
110   end
111   FRF_W(nf)=sum_Wl;
112 end
113 %% PLOT FLEXURAL FRF
114 figure(4) % FRF_W plots
115 subplot(2,2,1); plot(ff,real(FRF_W)); title('real FRF_W'); xlabel('f, kHz')
116 subplot(2,2,2); plot(ff,-imag(FRF_W)); title('-imag FRF_W'); xlabel('f, kHz')
117 subplot(2,2,3); plot(ff,abs(FRF_W)); title('abs FRF_W'); xlabel('f, kHz')
118 % set(gca,'Yscale','log');
119 subplot(2,2,4); plot(ff,180/pi*angle(FRF_W));...
120   title('angle FRF_W, deg'); xlabel('f, kHz')
121 %% COMBINE AXIAL AND FLEXURAL FRF
122 FRF=FRF_U+FRF_W; % combined freqeucy response functions
123 %% PLOT COMBINED FRF
124 figure(5) % FRF plots
125 subplot(2,2,1); plot(ff,real(FRF)); title('real FRF'); xlabel('f, kHz')
126 subplot(2,2,2); plot(ff,-imag(FRF)); title('-imag FRF'); xlabel('f, kHz')
127 subplot(2,2,3); plot(ff,abs(FRF)); title('abs FRF'); xlabel('f, kHz')
128 % set(gca,'Yscale','log');
129 subplot(2,2,4); plot(ff,180/pi*angle(FRF));...
130   title('angle FRF, deg'); xlabel('f, kHz')
131 %% STUCTURAL STIFFNESS and STIFFNESS RATIO
132 kSTR_=1./FRF; % freq-dependent complex structural stiffness
133 figure(16) % kSTR plots
134 subplot(2,2,1); plot(ff,real(kSTR_)); title('real kSTR'); xlabel('f, kHz')
135 subplot(2,2,2); plot(ff,imag(kSTR_)); title('imag kSTR'); xlabel('f, kHz')
136 subplot(2,2,3); plot(ff,abs(kSTR_)); title('abs kSTR'); xlabel('f, kHz')
137 % set(gca,'Yscale','log');
138 subplot(2,2,4); plot(ff,180/pi*angle(kSTR_));...
139   title('angle kSTR, deg'); xlabel('f, kHz')
140 figure(17) % superposed plot
141 plot(ff,real(kSTR_),ff,imag(kSTR_)); title('real kSTR, imag kSTR'); xlabel('f, kHz')
142 %% CALCULATE COMPLEX-NUMBER ELECTROMECHANICAL PWAS PROPERTIES
143 delta=1e-2; eta=1e-2; % PWAS mechanical damping and electrical loss factors
144 sE11_=(1-li*eta)*sE11; eT33_=(1-li*delta)*eT33; % complex PWAS mat. prop.
145 k31_2=d31^2/sE11_/eT33_; % complex coupling coefficient in PWAS material
146 C_=eT33_*ba*La/ta; % complex capacitance of the PWAS
147 c_=sqrt(1/pa/sE11_); % complex axial wave speed in PWAS
148 kPWAS_=ba*ta/sE11_/La; % complex stiffness of the PWAS
149 %% CALCULATE ADMITTANCE AND IMPEDANCE PLOTS
150 r_=kSTR_/kPWAS_ ; % freq-dependent complex stiffness ratio
151 phi_= w*La/2/c_; % frequency dependent complex phi
152 den=phi_.*cot(phi_)+r_; P1=1-1./den; P2=1-k31_2*P1;
153 Y=li.*w.*C_.*P2; Z=1./Y; % admittance and impedance

```

```
154 figure(18) % Y plots
155 subplot(2,2,1); plot(ff,real(Y));title('real Y'); xlabel('f, kHz')
156 subplot(2,2,2); plot(ff,imag(Y));title('imag Y'); xlabel('f, kHz')
157 subplot(2,2,3); plot(ff,abs(Y)); title('abs Y'); xlabel('f, kHz')
158 %      set(gca,'Yscale','log');
159 subplot(2,2,4); plot(ff,180/pi*angle(Y));...
160      title('angle Y, deg'); xlabel('f, kHz')
161 figure(19) % Z plots
162 subplot(2,2,1); plot(ff,real(Z));title('real Z'); xlabel('f, kHz')
163      set(gca,'Yscale','log');
164 subplot(2,2,2); plot(ff,imag(Z));title('imag Z'); xlabel('f, kHz')
165 subplot(2,2,3); plot(ff,abs(Z)); title('abs Z'); xlabel('f, kHz')
166 %      set(gca,'Yscale','log');
167 subplot(2,2,4); plot(ff,180/pi*angle(Y));...
168      title('angle Z, deg'); xlabel('f, kHz')
169 %% SUPERPOSED PLOT OF Y, Z, FRF
170 figure(20) % superposed plot
171 maxY=max(abs(real(Y))); maxZ=max(abs(real(Z))); maxFRF=max(abs(imag(FRF)));
172 plot(ff,real(Y)/maxY,ff,real(Z)/maxZ,ff,-imag(FRF)/maxFRF);
173 title('real(Y), real(Z), -imag(FRF)'); xlabel('f, kHz')
174      set(gca,'Yscale','log');
175 %      ylim([1e-3 1e0])
176      ylim([1e-2 1e0])
177
178
179
180
181
```

Problem 2: Consider again the data in Problem 1 above, but let either double the thickness ($h_2 = 5.2$ mm), or wider width ($b_2 = 19.6$ mm), or both. Use the 1-D analytical expressions deduced in this chapter to recalculate the admittance and impedance response of the PWAS in the interval 1 KHz to 30 kHz for these other combinations of thickness and width. Discuss your results

Solution

The rationale discussed in the previous problem applies here identically. The only things that change are the numerical values for the thickness and width. Hence, we distinguish four cases as discussed next.

Case 1: Narrow thin beam, $b_1 = 8$ mm, $h_1 = h_0 = 2.6$ mm .

This case was analyzed in Problem 10.1 above and need not be repeated here.

Case 2: Narrow thick beam, $b_2 = 8$ mm, $h_2 = 2h_0 = 5.2$ mm .

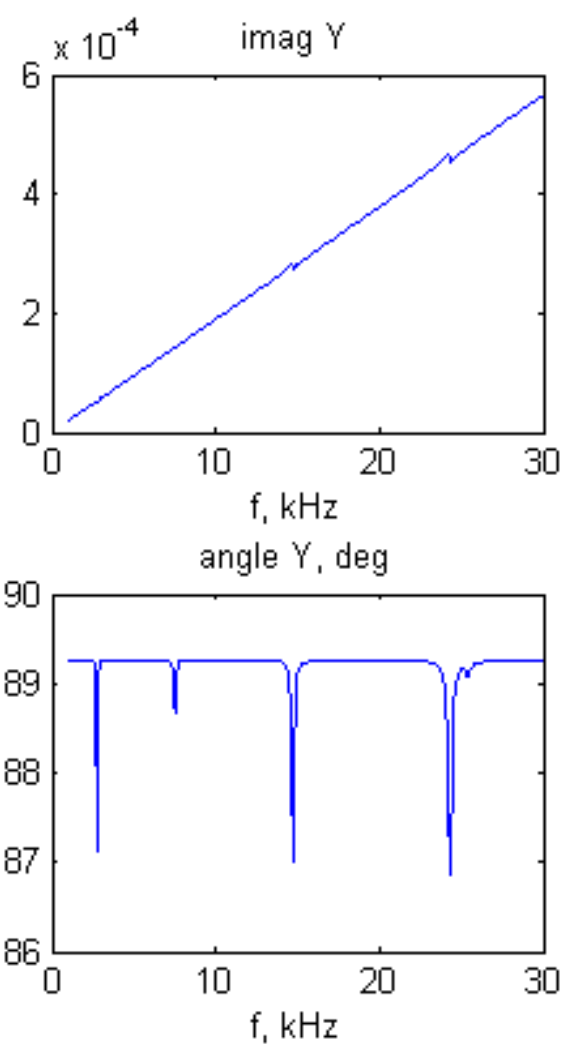
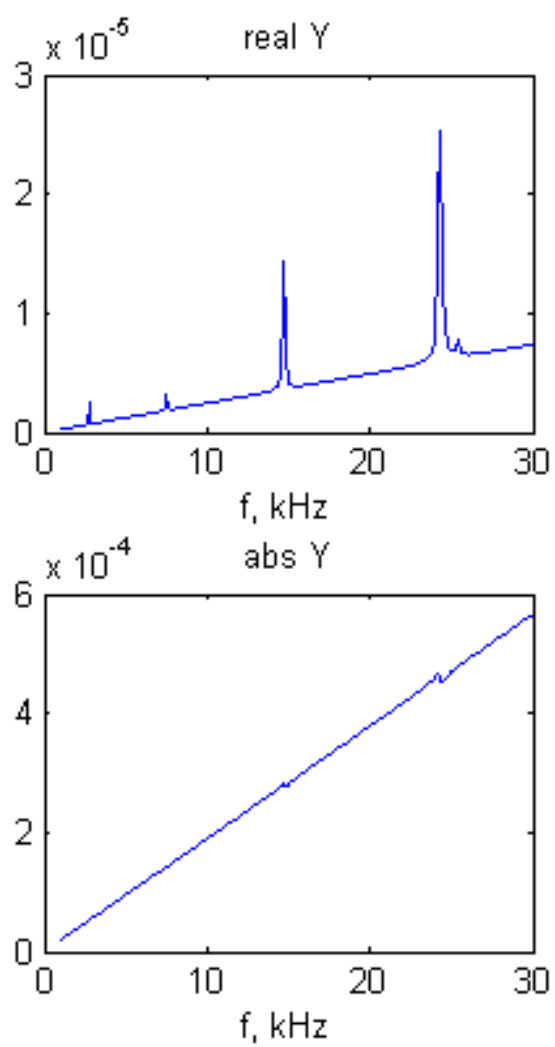
For the numerical values given in this problem, one obtains the following natural frequencies

Axial frequencies: $f_{j_u} = 25.4, 50.8$ kHz, $j_u = 1, 2$

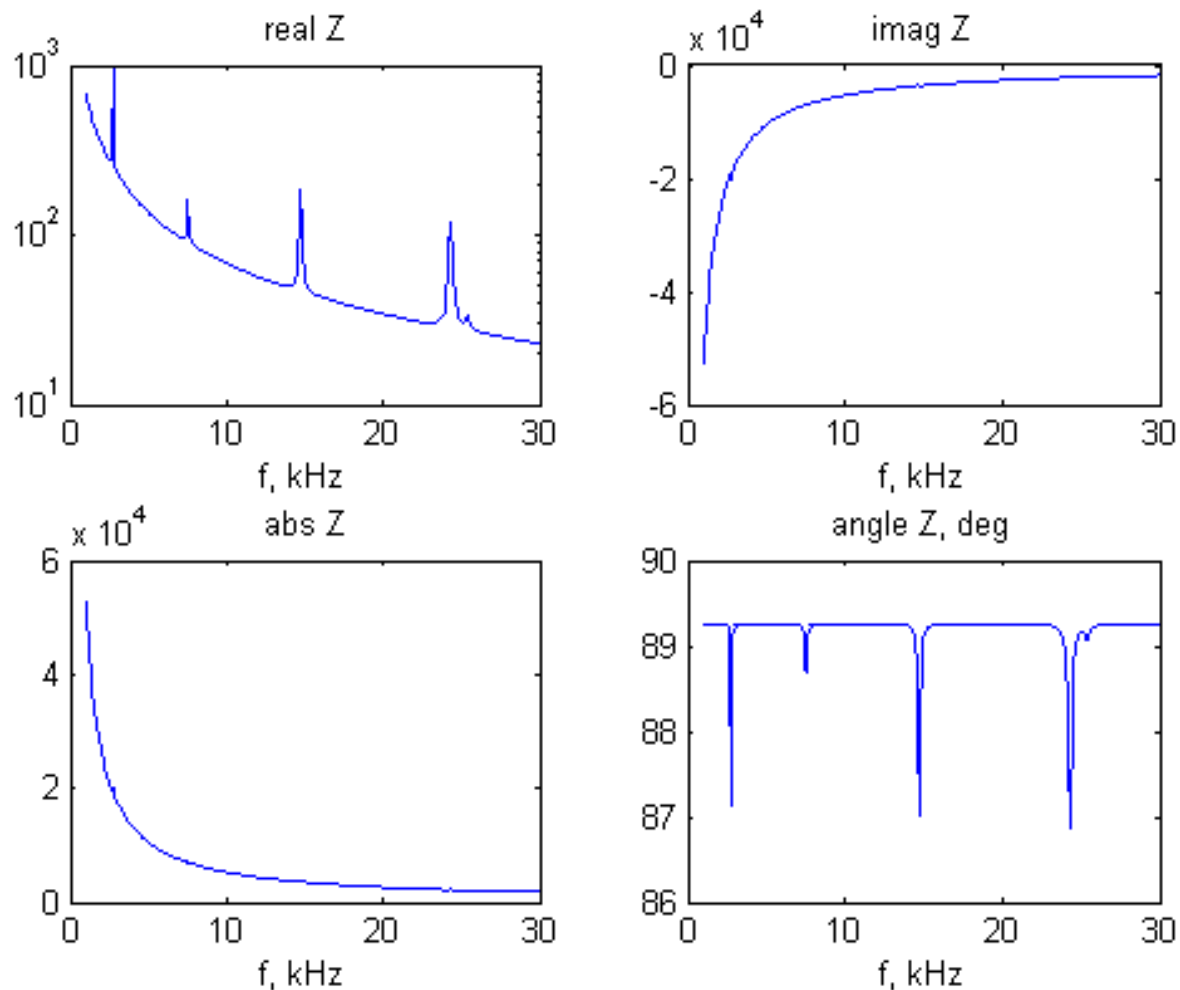
Flexural frequencies: $f_{j_w} = 2.72, 7.49, 14.67, 24.3, 36.2$ kHz, $j_w = 1, \dots, 4$

Again we have two close frequencies, the fourth flexural frequency $f_4^w = f_{4_w} = 24.3$ kHz and the first axial frequency $f_1^u = f_{1_u} = 25.4$ kHz . However, they are little better separated than in Case 1, hence we expect to distinguish a double peak in the spectrum.

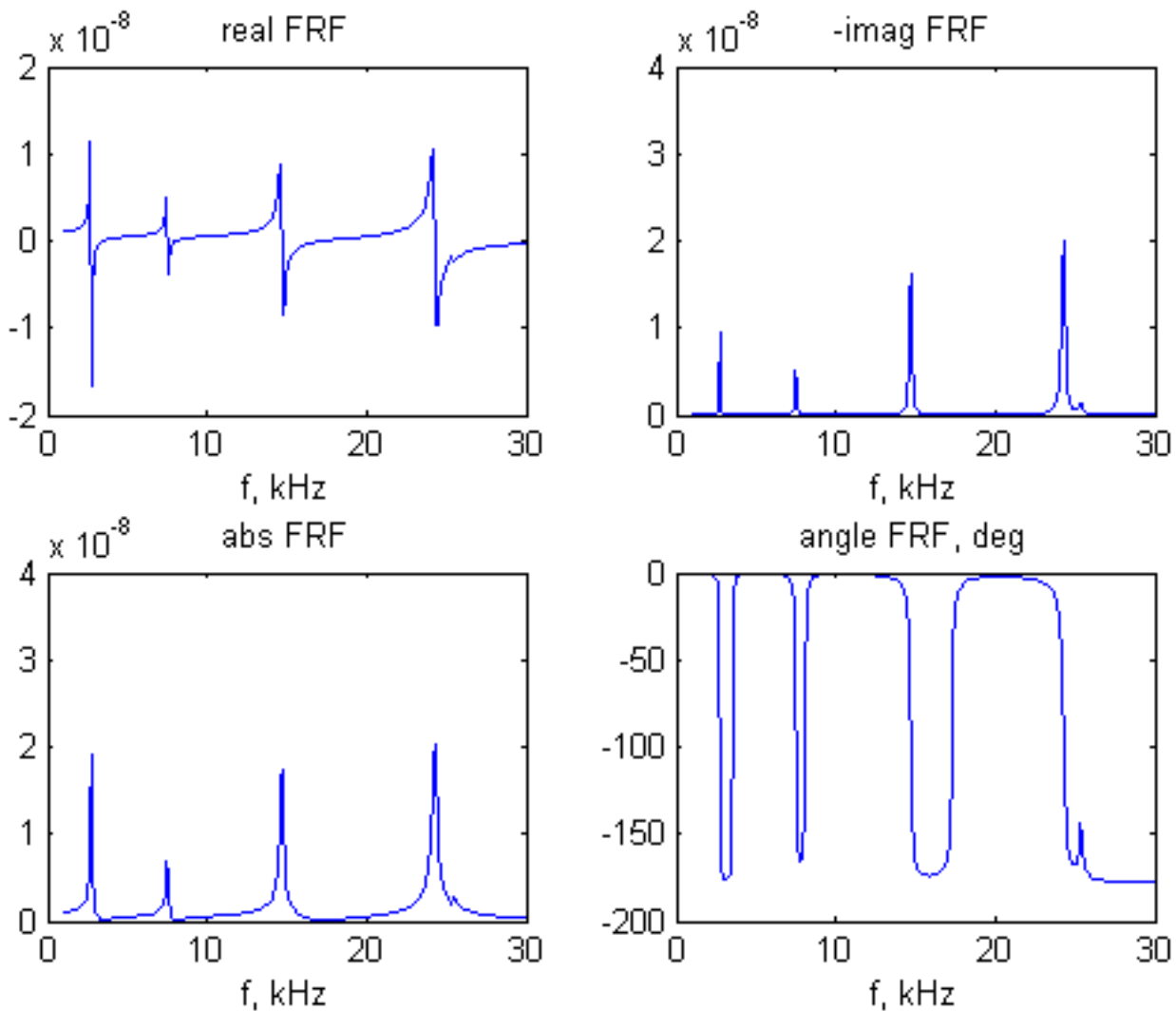
The admittance and impedance plots are as follows:



Impedance:

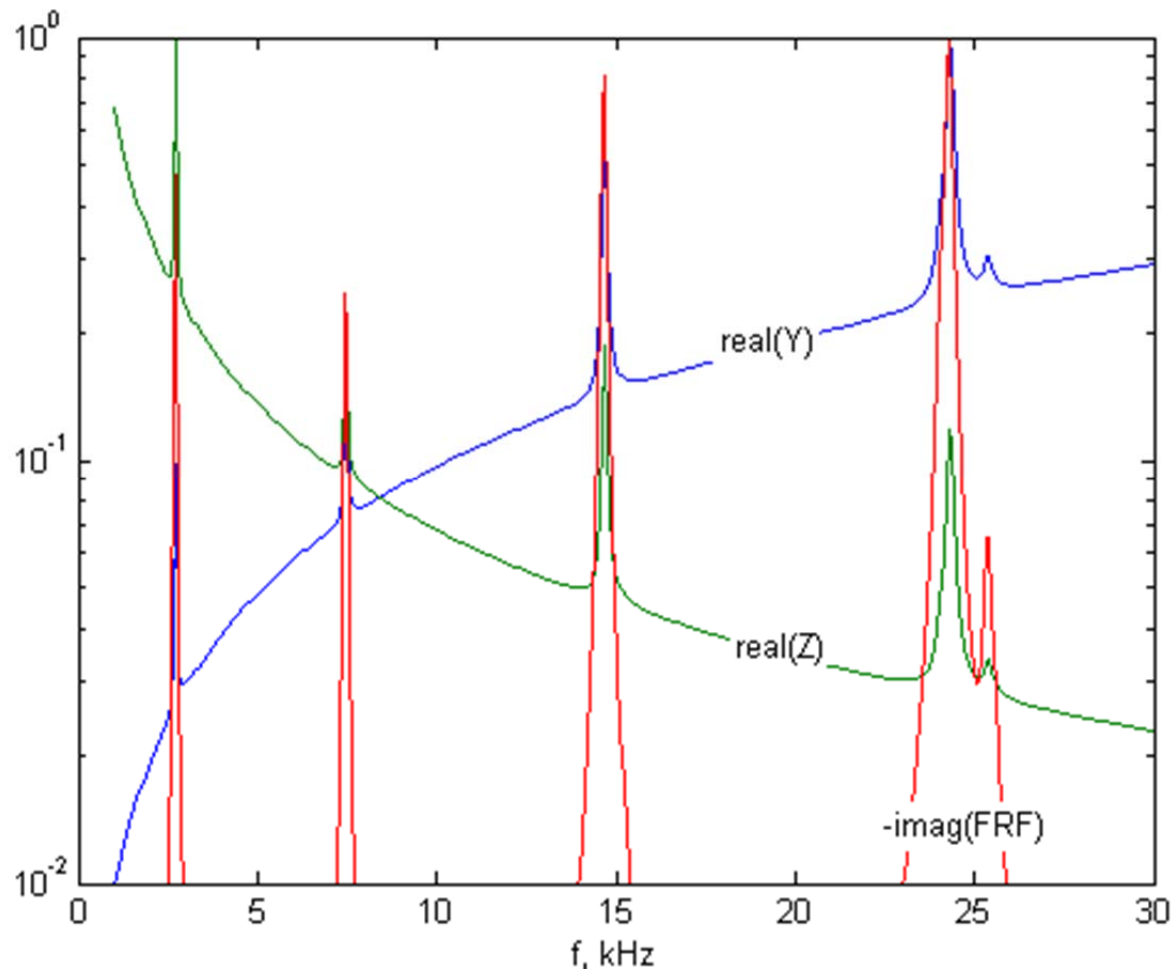


The FRF plot is given below.



The peaks of the FRF imaginary part correspond to resonance frequencies. In the frequency band of interest (1-30 kHz) there are five resonance frequencies ($f_1 = 2.72$ kHz, $f_2 = 7.49$ kHz, $f_3 = 14.67$ kHz, $f_4 = 24.26$ kHz, $f_5 = 25.4$ kHz). The first four frequencies are due to flexural vibration, the last is due to axial vibration. The twin peak behavior at the right hand end of the spectrum is due to the proximity between the last two resonances in the spectrum, $f_4^w = 24.3$ kHz and $f_1^u = 25.4$ kHz.

The superposed plots (with appropriate scale factors) of the admittance and impedance real parts and the frequency response function imaginary part are given next.



One observes that the peaks of the three curves represented in these plots align perfectly. This indicates that the admittance and impedance real parts follow with fidelity the structural resonances as depicted by the structural frequency response function at the PWAS location.

1

+ Ch.10 Problems 10.1, 10.2 (steel beams) ...

5

- % DEFINE PROPERTIES

6

- mm=1e-3; L=100*mm; b0=8*mm; h0=2.6*mm; E=200e9; p=7750; % steel beam

7

% b=b0; h=h0; % Problem 10.1 and Problem 10.2 Case 1

8

b=b0; h=2*h0; % Problem 10.2 Case 2 narrow thick beam

9

% b=19.6*mm; h=h0; % Problem 10.2 Case 3 wide thin beam

16

10

% b=19.6*mm; h=2*h0; % Problem 10.2 Case 4 wide thick beam

Case 3: Wide thin beam, $b_3 = 19.6$ mm, $h_3 = h_0 = 2.6$ mm.

For the numerical values given in this problem, one obtains the following natural frequencies

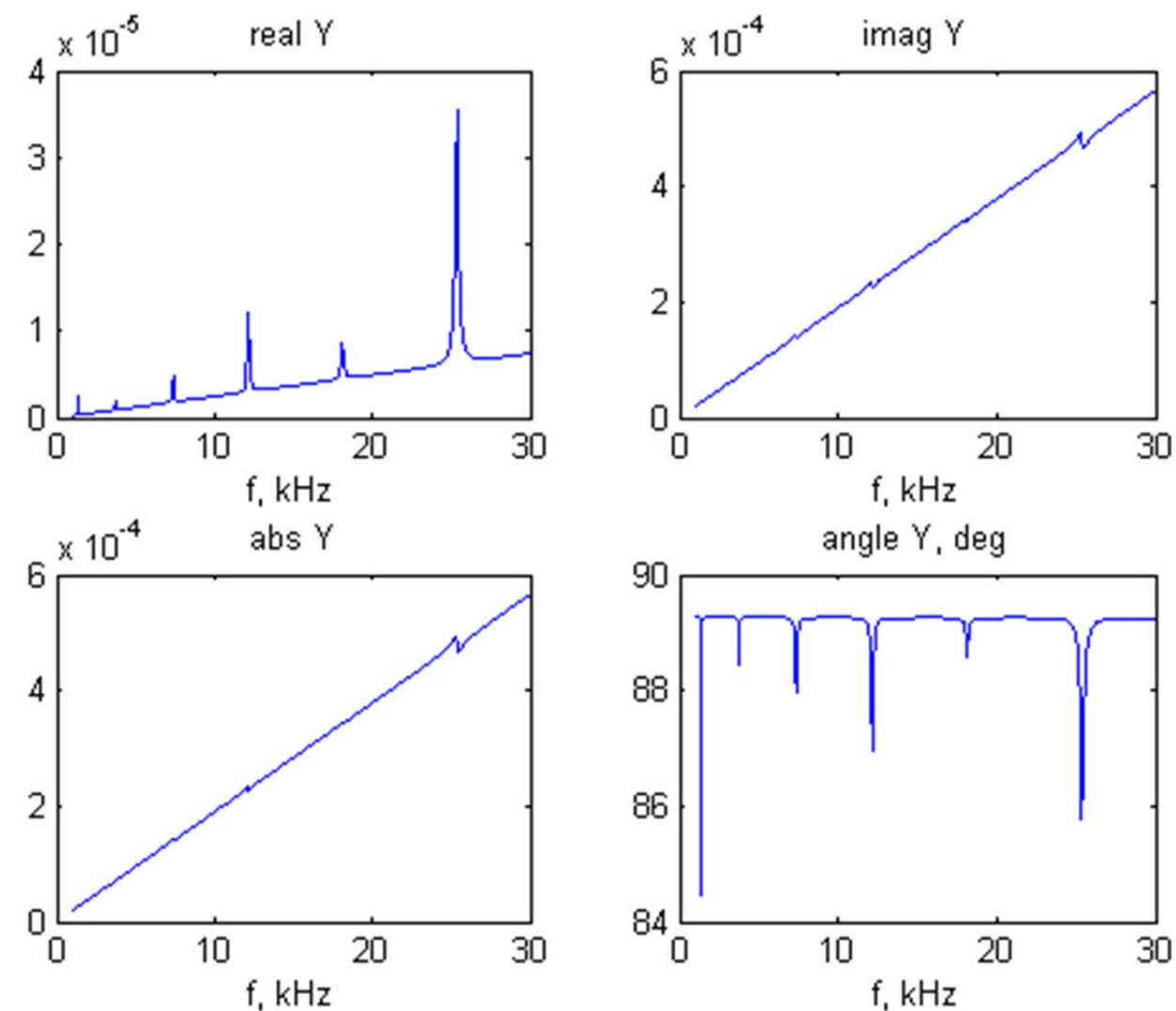
Axial frequencies: $f_{j_u} = 25.4, 50.8$ kHz, $j_u = 1, 2$

Flexural frequencies: $f_{j_w} = 1.358, 3.74, 7.34, 12.13, 18.12, 25.3$ kHz, $j_w = 1, \dots, 6$

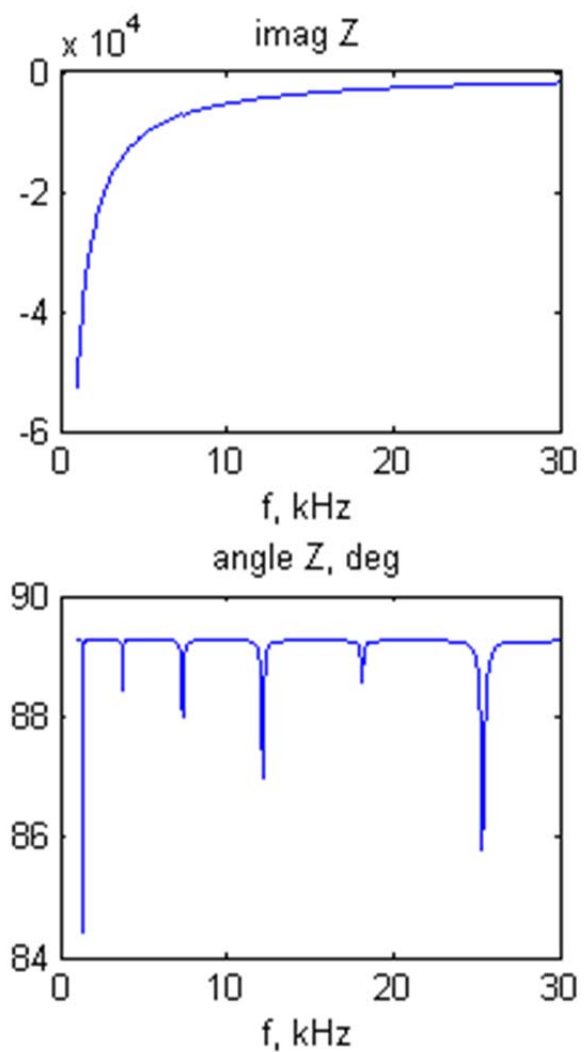
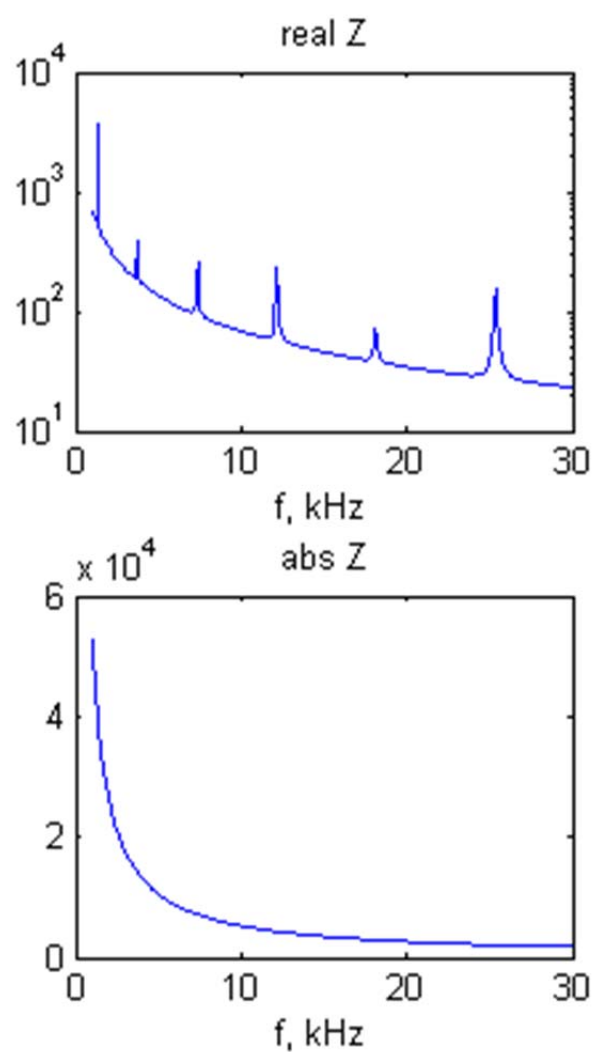
Again we have two very close frequencies, the first axial frequency $f_1^u = f_{1_u} = 25.4$ kHz and the sixth flexural frequencies $f_6^w = f_{6_w} = 25.3$ kHz. This fact will produce again overlap of the peaks in the plots.

The admittance and impedance plots are as follows:

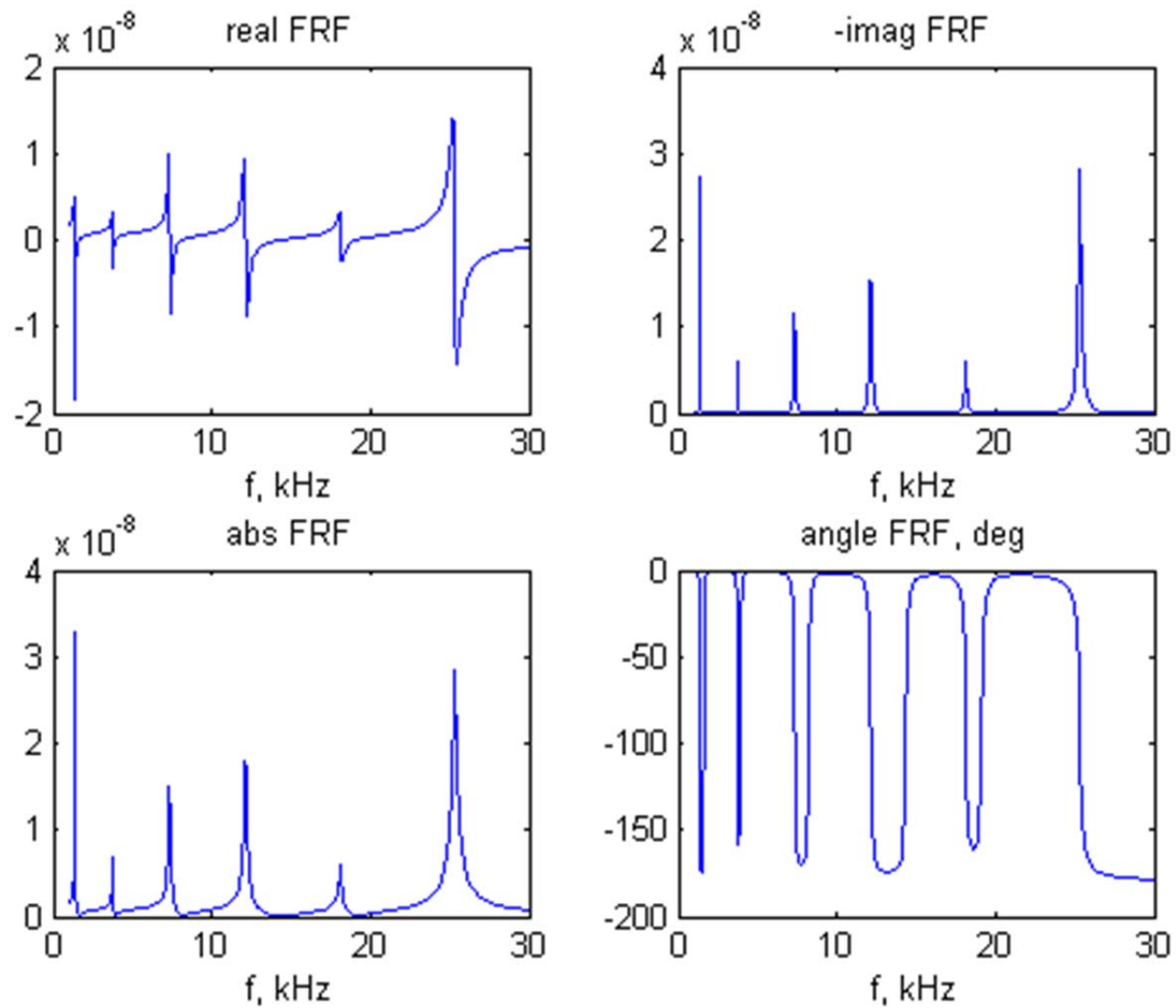
Admittance:



Impedance:

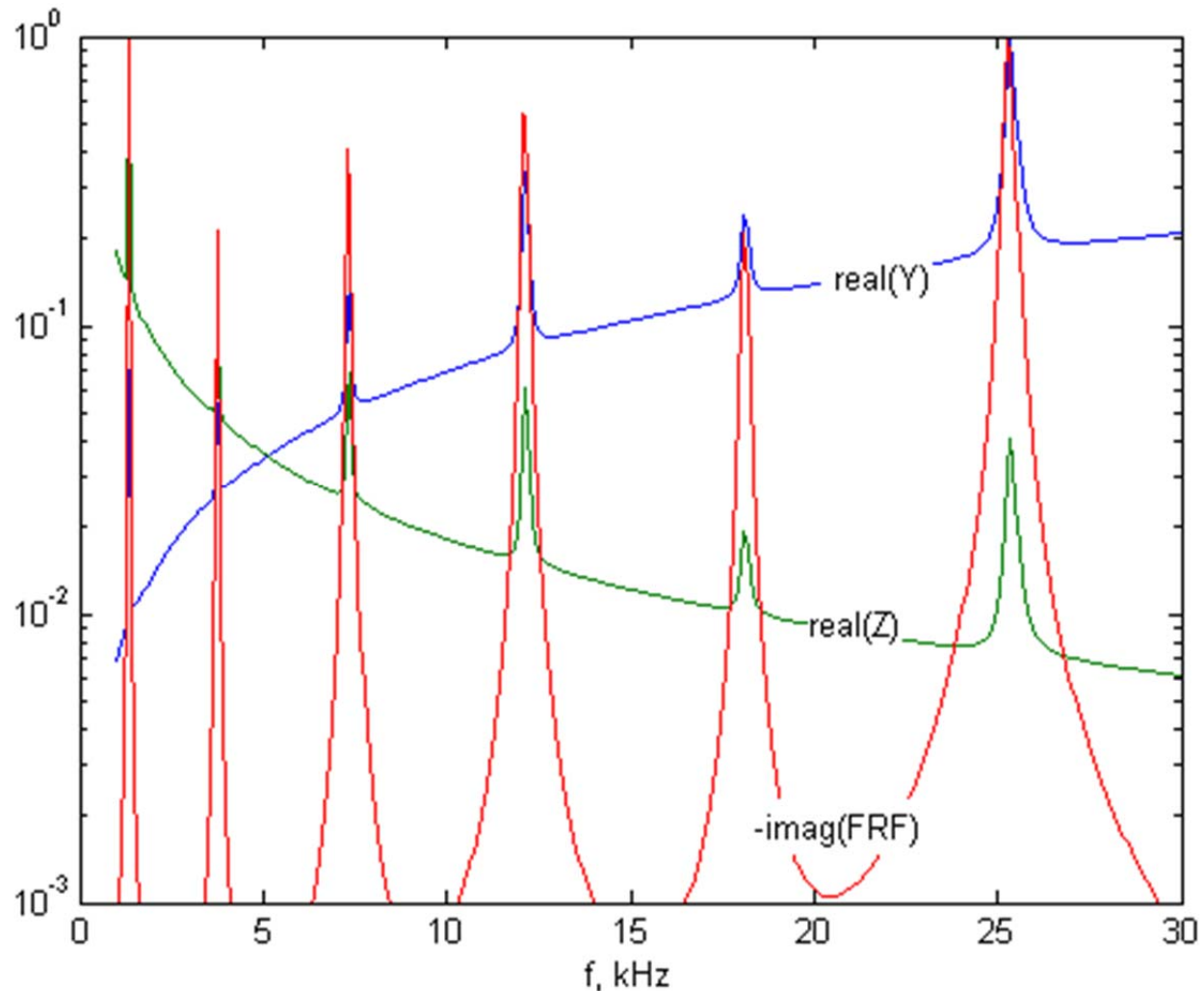


The FRF plot is given next.



The peaks of the FRF imaginary part correspond to resonance frequencies. In the frequency band of interest (1-30 kHz) there are six resonance frequencies ($f_1 = 1.36$ kHz, $f_2 = 3.74$ kHz, $f_3 = 7.34$ kHz, $f_4 = 12.13$ kHz, $f_5 = 18.12$ kHz, $f_6 = 25.4$ kHz). The first five frequencies are due to flexural vibration, whereas the sixth is due to an overlap of the first axial resonance ($f_1^u = 25.4$ kHz) and the sixth flexural resonance ($f_6^w = 25.3$ kHz).

The superposed plots (with appropriate scale factors) of the admittance and impedance real parts and the frequency response function imaginary part are given next.



One observes that the peaks of the three curves represented in these plots align perfectly. This indicates that the admittance and impedance real parts follow with fidelity the structural resonances as depicted by the structural frequency response function at the PWAS location.

5 - % DEFINE PROPERTIES

6 mm=1e-3; L=100*mm; b0=8*mm; h0=2.6*mm; E=200e9; p=7750; % steel beam

7 % b=b0; h=h0; % Problem 10.1 and Problem 10.2 Case 1

8 % b=b0; h=2*h0; % Problem 10.2 Case 2 narrow thick beam

9 b=19.6*mm; h=h0; % Problem 10.2 Case 3 wide thin beam 21

10 % b=19.6*mm; h=2*h0; % Problem 10.2 Case 4 wide thick beam

Case 4: Wide thick beam, $b_4 = 19.6$ mm, $h_4 = 2h_0 = 5.2$ mm.

For the numerical values given in this problem, one obtains the following natural frequencies

Axial frequencies: $f_{j_u} = 25.4, 50.8$ kHz, $j_u = 1, 2$

Flexural frequencies: $f_{j_w} = 2.72, 7.49, 14.67, 24.3, 36.2$ kHz, $j_w = 1, \dots, 4$

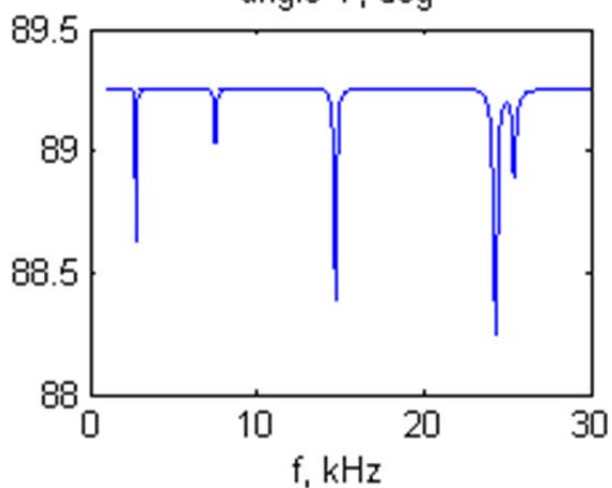
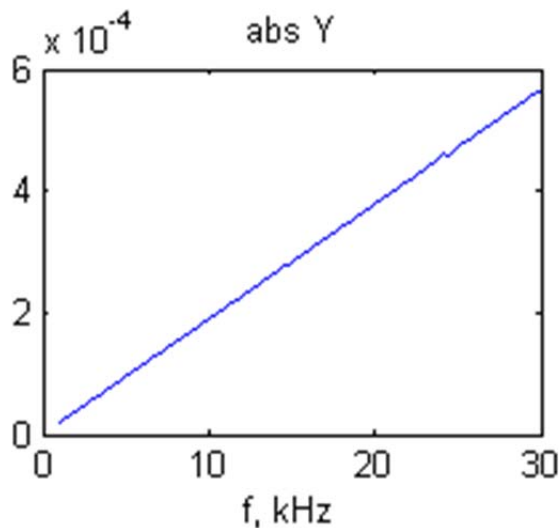
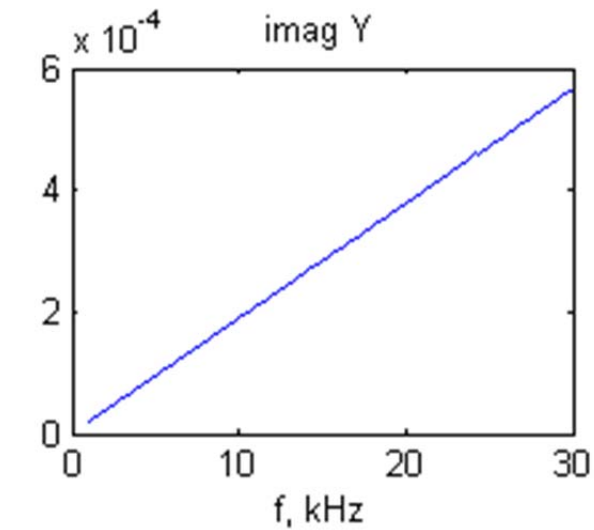
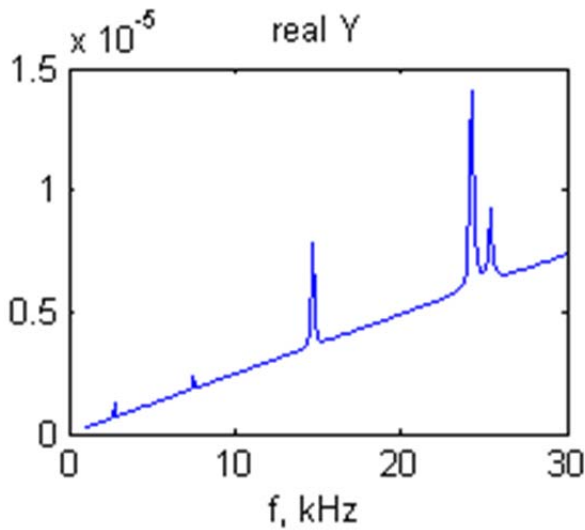
Again we have two close frequencies, the fourth flexural frequency $f_4^w = f_{4_w} = 24.3$ kHz and

the first axial frequency $f_1^u = f_{1_u} = 25.4$ kHz. However, they are little better separated than in

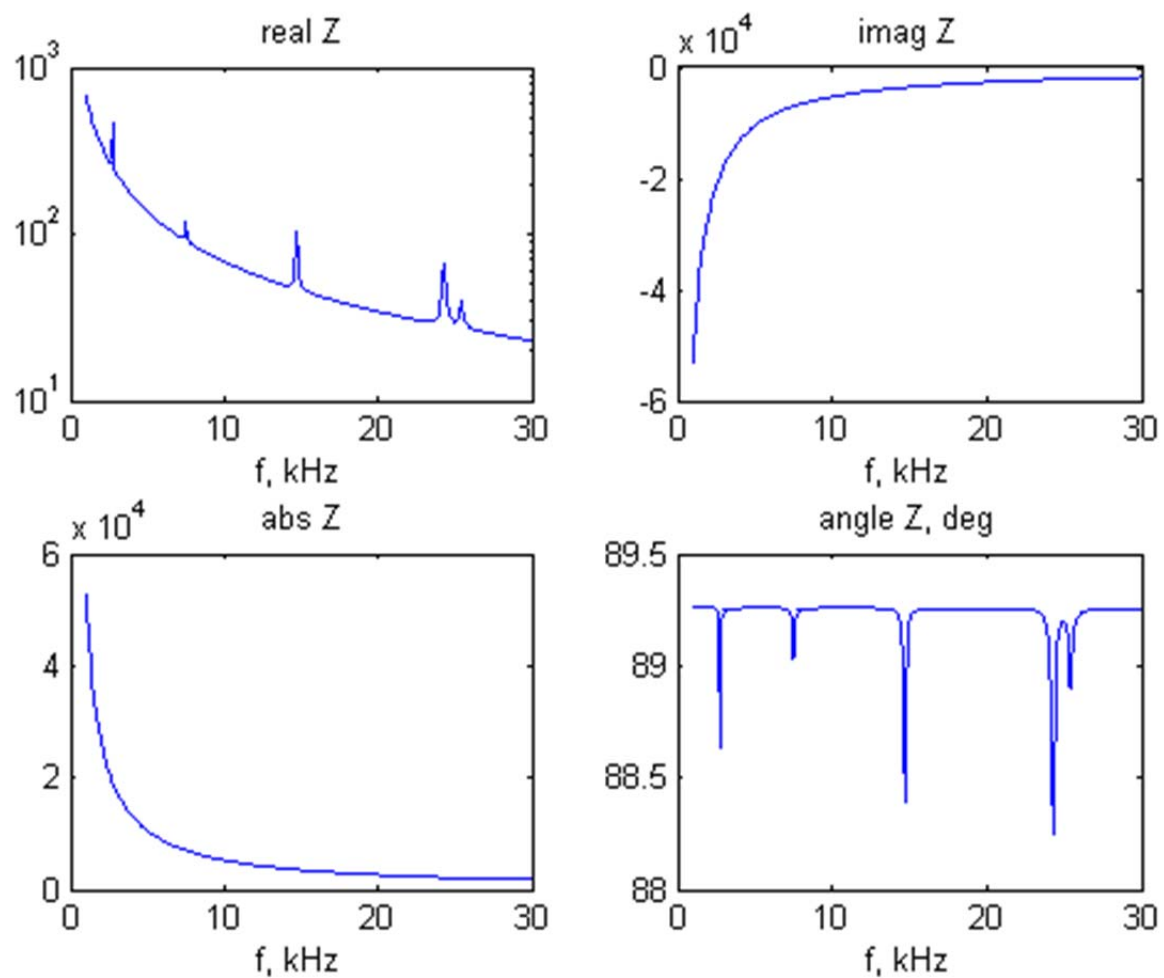
Case 1 and Case 3, hence we expect to distinguish a double peak in the spectrum.

The admittance and impedance plots are as follows:

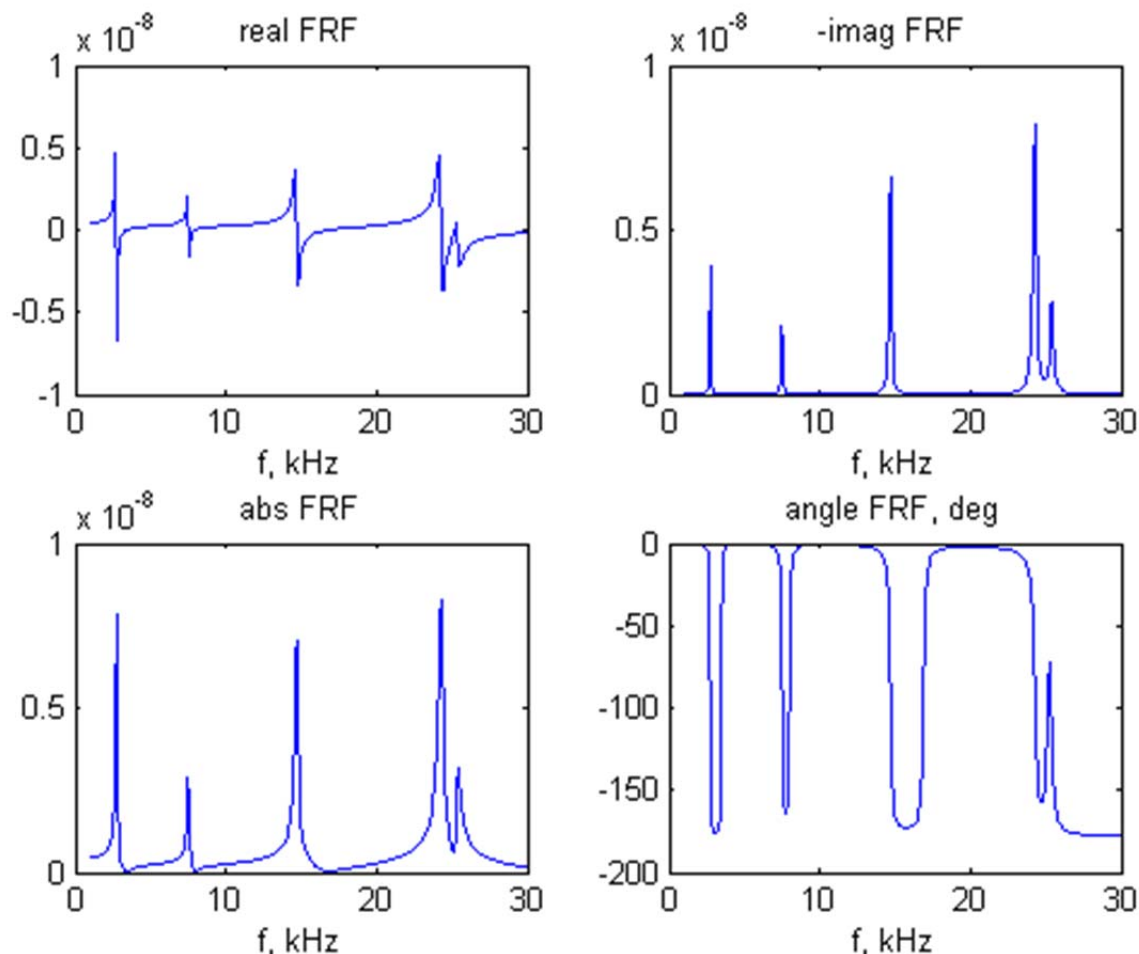
Admittance:



Impedance:

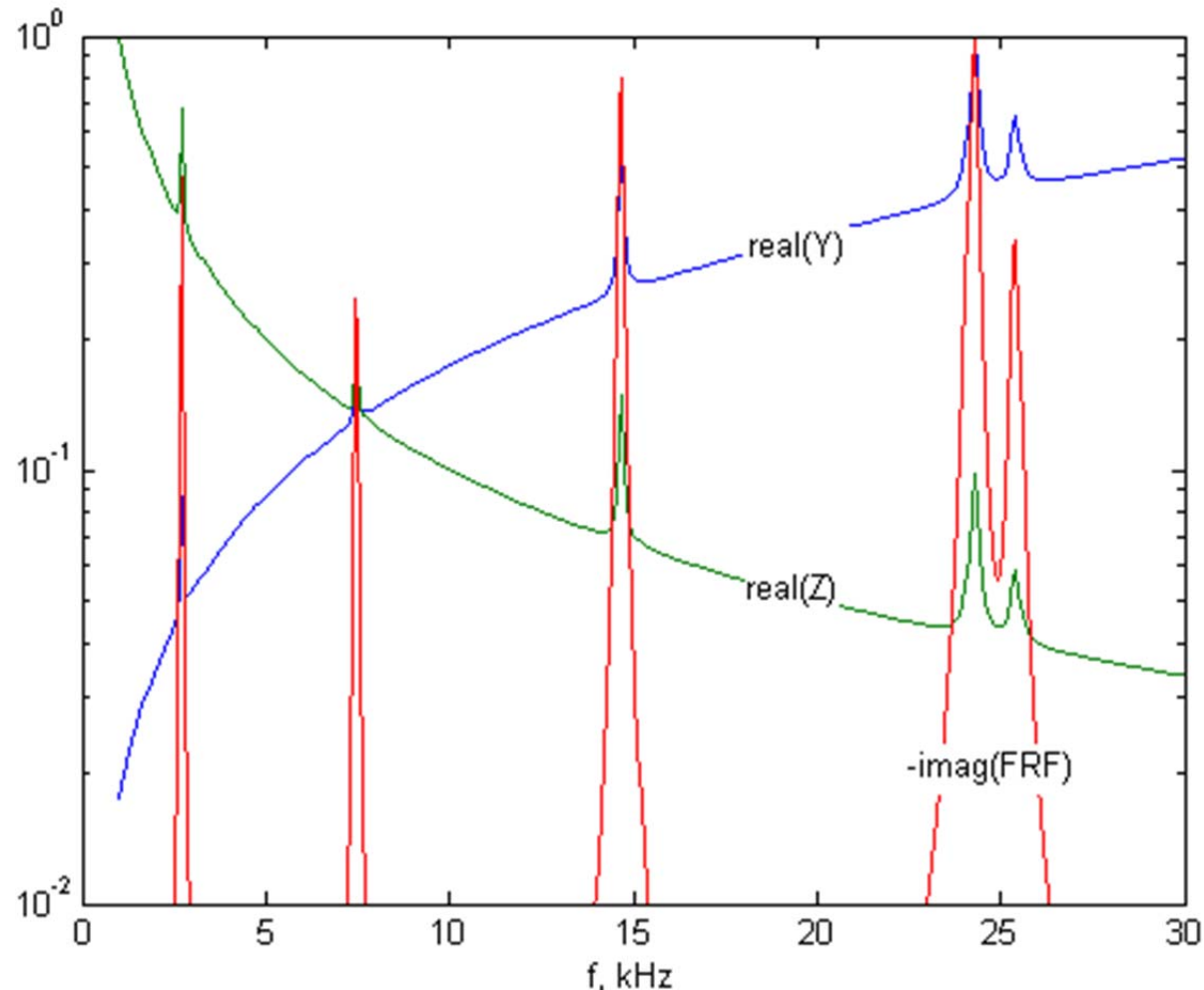


The FRF plot is given below.



The peaks of the FRF imaginary part correspond to resonance frequencies. In the frequency band of interest (1-30 kHz) there are five resonance frequencies ($f_1 = 2.72$ kHz, $f_2 = 7.48$ kHz, $f_3 = 14.67$ kHz, $f_4 = 24.26$ kHz, $f_5 = 25.4$ kHz). The first four frequencies are due to flexural vibration, the last is due to axial vibration. The twin peak behavior at the right hand end of the spectrum is due to the proximity between the last two resonances in the spectrum, $f_4^w = 24.3$ kHz and $f_5^u = 25.4$ kHz.

The superposed plots (with appropriate scale factors) of the admittance and impedance real parts and the frequency response function imaginary part are given next.



One observes that the peaks of the three curves represented in these plots align perfectly. This indicates that the admittance and impedance real parts follow with fidelity the structural resonances as depicted by the structural frequency response function at the PWAS location.

1 + % Ch.10 Problems 10.1, 10.2 (steel beams) %..%

5 - % DEFINE PROPERTIES

6 - mm=1e-3; L=100*mm; b0=8*mm; h0=2.6*mm; E=200e9; p=7750; % steel beam

7 % b=b0; h=h0; % Problem 10.1 and Problem 10.2 Case 1

8 % b=b0; h=2*h0; % Problem 10.2 Case 2 narrow thick beam

9 % b=19.6*mm; h=h0; % Problem 10.2 Case 3 wide thin beam

10 b=19.6*mm; h=2*h0; % Problem 10.2 Case 4 wide thick beam

Problem 3: Consider a circular aluminum plate of thickness 0.8 mm, diameter 100 mm, and material properties given in Table 10.1. A 7-mm circular PWAS ($r_a = 7$ mm, $t_a = 0.2$ mm) is bonded in the center of the plate. The material properties of the PWAS are given in Table 10.2. Assume 1% mechanical damping and electric loss. (i) Use the 2-D analytical expressions deduced in this chapter to calculate the admittance and impedance response in the interval 1 KHz to 40 kHz of the PWAS attached to the structure. (Hint: use Eqs. (84), (85)). (ii) Plot superposed on the same chart (with appropriate scale factors) the admittance and impedance real parts and the frequency response function imaginary part. Comment on the significance of the peaks observed in these plots.

Solution

To calculate the admittance and impedance response of the circular PWAS attached to the structure, use the constraint PWAS expression for $Z(\omega)$ given in textbook Eqs. (10.84), (10.85), i.e.,

$$Y(\omega) = i\omega \bar{C} \left\{ 1 - \bar{k}_p^2 \left[1 - \frac{(1+\nu_a) J_1(\bar{\phi})}{\bar{\phi} J_0(\bar{\phi}) - [(1-\nu_a) - (1+\nu_a) \bar{\chi}(\omega)] J_1(\bar{\phi})} \right] \right\} \quad (10.84) \text{ (1)}$$

Inversion of the impedance $Z(\omega)$ yields the admittance $Y(\omega) = Z^{-1}(\omega)$, i.e.,

$$Z(\omega) = Y^{-1}(\omega) = \frac{1}{i\omega \bar{C}} \left\{ 1 - \bar{k}_p^2 \left[1 - \frac{(1+\nu_a) J_1(\bar{\phi})}{\bar{\phi} J_0(\bar{\phi}) - [(1-\nu_a) - (1+\nu_a) \bar{\chi}(\omega)] J_1(\bar{\phi})} \right] \right\}^{-1} \quad (10.85) \text{ (2)}$$

where

$$\bar{C} = \bar{\epsilon}_{33}^T \frac{\pi r_a^2}{t_a} \quad (\text{complex capacitance of the PWAS}) \quad (10.86) \text{ (3)}$$

$$\bar{k}_p^2 = \frac{2}{(1-\nu_a)} \frac{d_{31}^2}{\bar{s}_{11}^E \bar{\epsilon}_{33}^T} \quad (\text{complex planar coupling coefficient in PWAS material}) \quad (10.87) \text{ (4)}$$

$$\bar{\phi} = r_a \frac{\omega}{\bar{c}_a} \quad (\text{complex phase angle in PWAS material}) \quad (10.88) \text{ (5)}$$

$$\bar{c}_a = \sqrt{\frac{1}{\rho_a \bar{s}_{11}^E (1-\nu_a^2)}} , \quad (\text{complex in-plane wave speed in PWAS}) \quad (10.89) \text{ (6)}$$

$$\bar{\epsilon}_{33} = \epsilon_{33} (1-i\delta) \quad (\text{complex electric permittivity in the PWAS material}) \quad (10.90) \text{ (7)}$$

$$\bar{s}_{11}^E = s_{11}^E (1-i\eta) \quad (\text{complex mechanical compliance in the PWAS material}) \quad (10.91) \text{ (8)}$$

with ν_a being the Poisson ratio in the PWAS material. The mechanical damping ratio η and the electrical damping ratio δ vary with the formulation of the piezoceramic PWAS material, but are usually small ($\eta, \delta < 5\%$). A brief derivation of this formula is given in the textbook Section 10.3 of Chapter 10. The stiffness ratio, $\bar{\chi}(\omega)$, is calculated with textbook Eqs. (10.92), i.e.,

$$\bar{\chi}(\omega) = \frac{\bar{k}_{str}(\omega)}{\bar{k}_{PWAS}} \quad (10.92) (9)$$

where $\bar{k}_{str}(\omega)$ is the structural stiffness given by Eq. (8.83)

$$\bar{k}_{str}(\omega) = \frac{\rho ha^2}{2r_a} \left[\sum_{j_u=N_u^{low}}^{N_u^{high}} \frac{U_{j_u}^2(r_a)}{-\omega^2 + 2i\zeta_{j_u}\omega\omega_{j_u} + \omega_{j_u}^2} + \left(\frac{h}{2}\right)^2 \sum_{j_w=N_w^{low}}^{N_w^{high}} \frac{W_{j_w}^{\prime 2}(r_a)}{-\omega^2 + 2i\zeta_{j_w}\omega\omega_{j_w} + \omega_{j_w}^2} \right]^{-1} \quad (8.83) (10)$$

The expression \bar{k}_{PWAS} is the complex PWAS stiffness given by Eq. (8.93), i.e.,

$$\bar{k}_{PWAS} = \frac{t_a}{r_a \bar{s}_{11}^E (1-\nu_a)}, \quad (\text{complex PWAS stiffness}) \quad (8.93) (11)$$

with t_a being the PWAS thickness. The frequency-dependent structural dynamic stiffness, $\bar{k}_{str}(\omega)$ of Eq. (10), is calculated by performing the dynamic analysis of the circular plate undergoing forced vibration under PWAS excitation. This analysis (which is an extension of the elastic plate vibration analysis of Chapter 4) is presented in detail in the textbook Section 10.3.1 through Section 10.3.3, and will not be repeated here.

Equation (7) involves the use of the axial and flexural vibration modeshapes of free circular plates given by Eqs. (10.55)–(10.58) for axial vibration and Eqs. (10.64)–(10.68) for flexural vibration, i.e.,

$$U_{j_u}(r) = A_{j_u} J_1(\gamma_{j_u} r) \quad \gamma_{j_u} = z_{j_u}/a \quad (\text{axial modes}) \quad (10.55) (12)$$

$$A_{j_u} = 1/\sqrt{J_1^2(z_{j_u}) - J_0(z_{j_u})J_2(z_{j_u})} \quad (\text{axial amplitudes}) \quad (10.56) (13)$$

$$\frac{z_{j_u} J_0(z_{j_u})}{J_1(z_{j_u})} = (1-\nu) \Rightarrow z_{j_u} J_0(z_{j_u}) - (1-\nu) J_1(z_{j_u}) = 0 \quad (\text{axial char. eq.}) \quad (10.57) (14)$$

$$W_{j_w}(r) = A_{j_w} [J_0(\gamma_{j_w} r) + C_{j_w} I_0(\gamma_{j_w} r)] \quad \gamma_{j_w} = z_{j_w}/a \quad (\text{flexural modes}) \quad (10.64) (15)$$

$$\frac{z_{j_w} J_0(z_{j_w}) - (1-\nu) J_1(z_{j_w})}{z_{j_w} I_0(z_{j_w}) - (1-\nu) I_1(z_{j_w})} + \frac{J_1(z_{j_w})}{I_1(z_{j_w})} = 0 \quad (\text{flex. char. eq.}) \quad (10.65) (16)$$

$$C_{j_w} = -J_1(z_{j_w})/I_1(z_{j_w}) \quad (\text{flexural coefficients}) \quad (10.67) (17)$$

$$A_{j_w} = \frac{a}{\sqrt{2}} \sqrt{\int_0^a [J_0(z_{j_w} r/a) + C_{j_w} I_0(z_{j_w} r/a)]^2 r dr} \quad (\text{flexural amplitudes}) \quad (10.68) (18)$$

The derivative of the flexural mode Eq. (15) is obtained as follows: write Eq. (15) in generic way with the notation $\gamma = z/a$, i.e.,

$$w(r) = W(r)/A = J_0(\gamma r) + CI_0(\gamma r) \quad (\text{generic flexural modes}) \quad (10.64) (19)$$

Differentiate Eq. (19) w.r.t. r to get

$$w'(r) = \gamma J'_0(\gamma r) + \gamma C I'_0(\gamma r) \quad (\text{derivative of generic flexural modes}) \quad (20)$$

Recall the relations between Bessel functions and their derivatives as given by Eqs. (A.143), (A.159) of Appendix A, i.e.,

$$J'_0(x) = -J_1(x) \quad (\text{A.143}) \quad (21)$$

$$I'_0(x) = I_1(x) \quad (\text{A.159}) \quad (22)$$

Substitute Eqs. (21), (22) into Eq. (20) to get

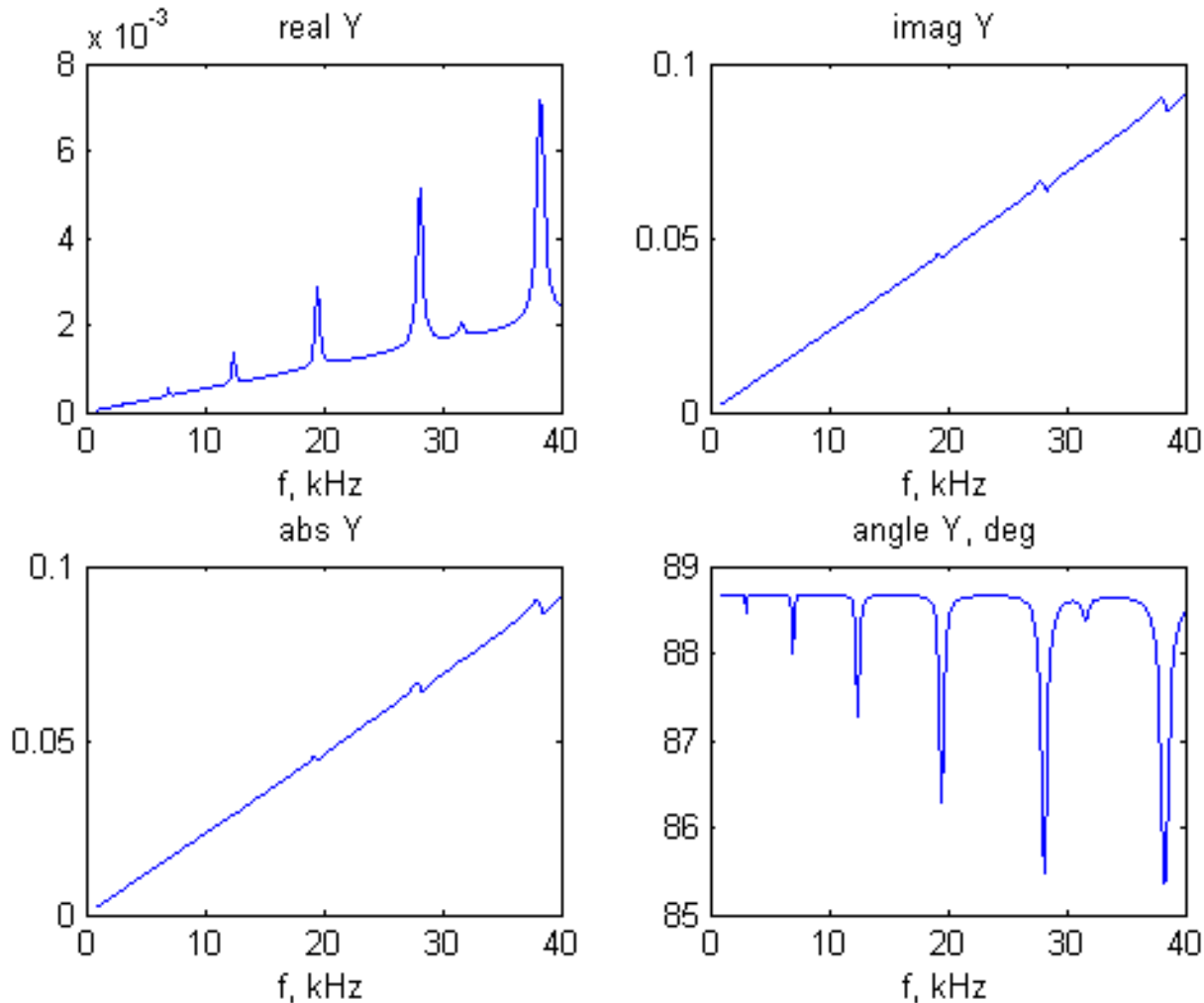
$$w'(r) = -\gamma J_1(\gamma r) + \gamma C I_1(\gamma r) \quad (23)$$

Use Eq. (23) to write the derivative of Eq. (15) as

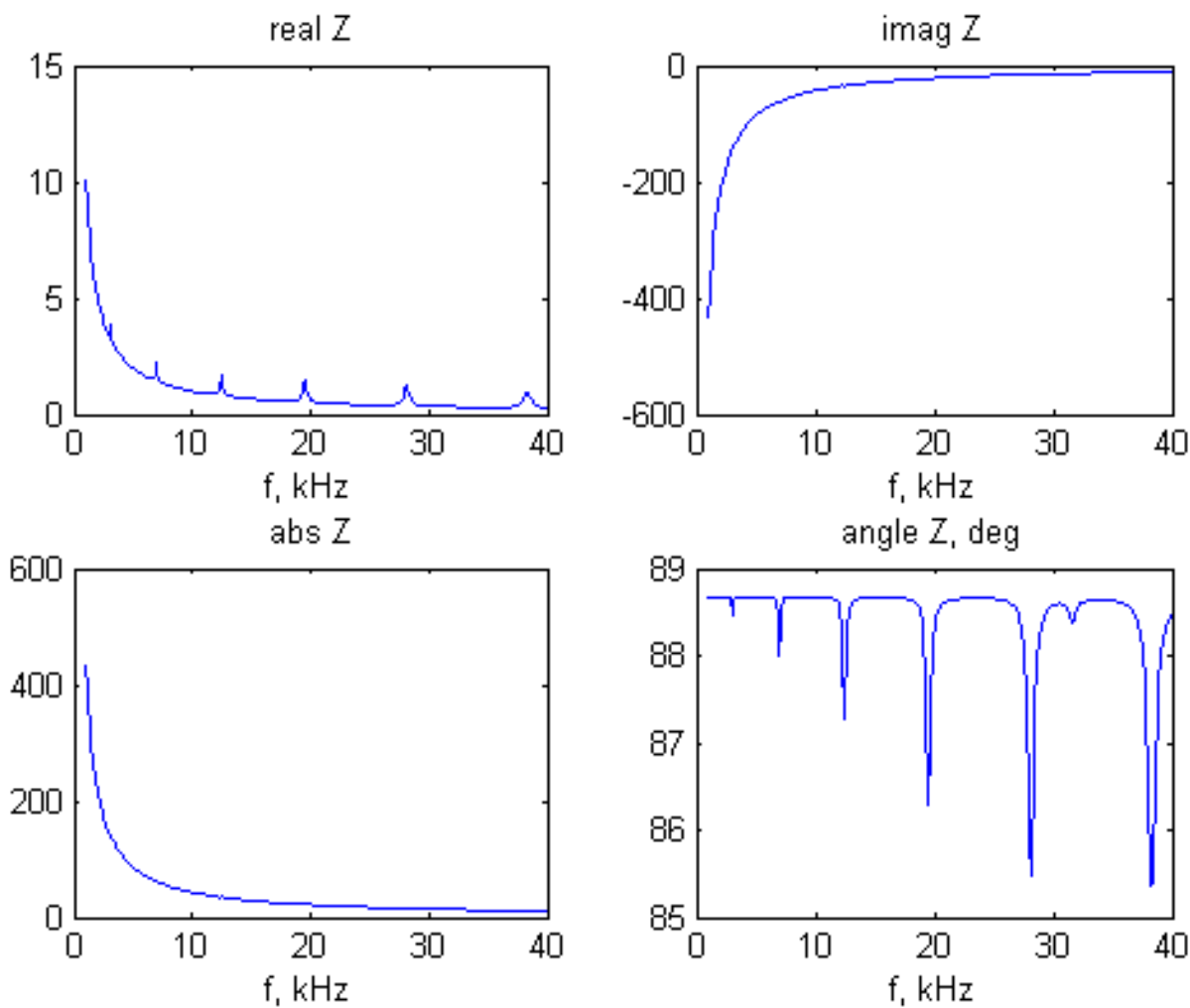
$$W'_{j_w}(r) = A_{j_w} \gamma_{j_w} \left[-J_1(\gamma_{j_w} r) + C_{j_w} I_1(\gamma_{j_w} r) \right] \quad \gamma_{j_w} = z_{j_w}/a \quad (\text{slope of flex. modes}) \quad (24)$$

(i) Using the given numerical values and taking the structural damping same as the mechanical damping ($\zeta_{j_u} = \zeta_{j_w} = \eta$), we get the following admittance and impedance plots:

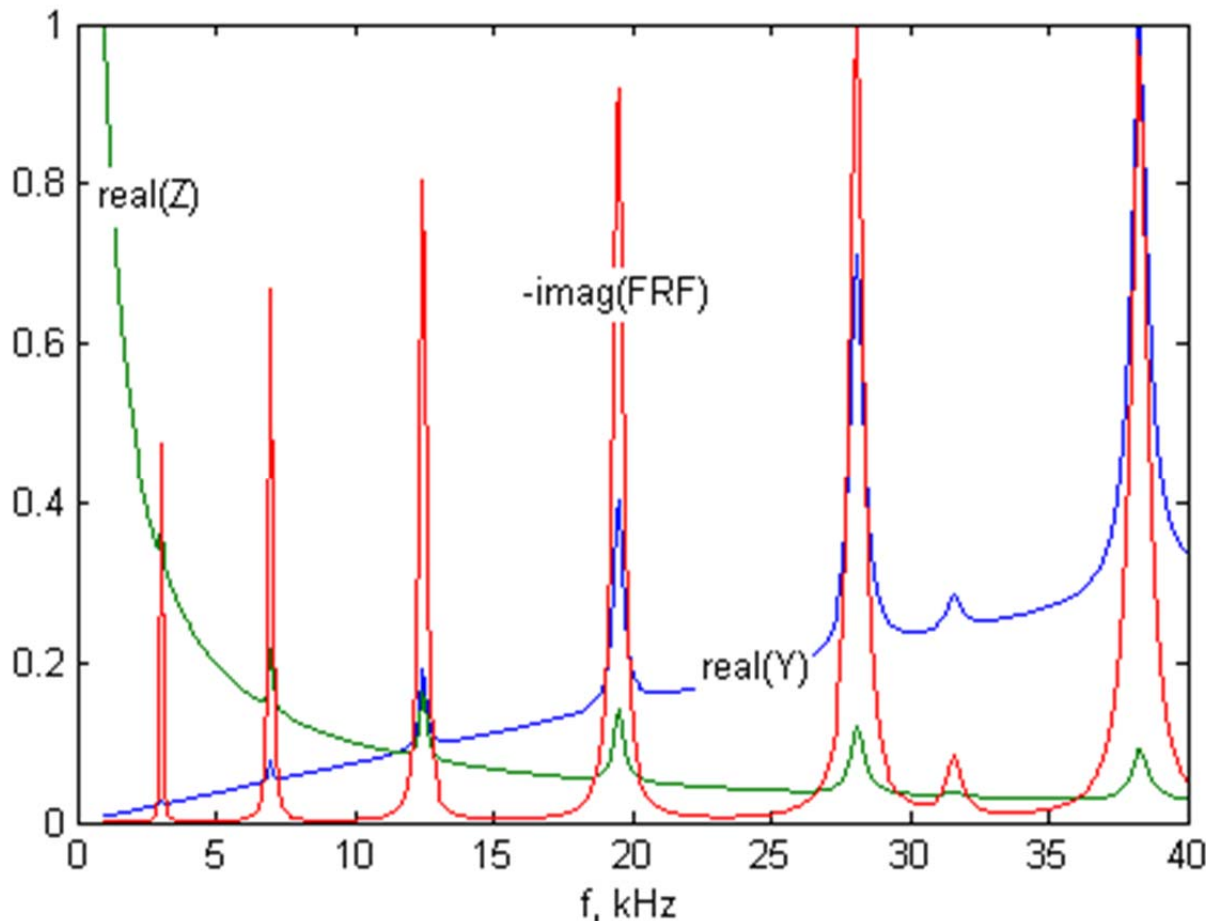
Admittance plot:



Impedance plot:



(ii) The superposed plot (with appropriate scale factors) of the admittance real part, $\text{real}(Y)$, impedance real part, $\text{real}(Z)$, and frequency response function imaginary part, $-\text{imag}(FRF)$ is shown below.



Comment: The peaks observed in these plots correspond to the natural frequencies of axial and flexural vibration of the circular plate $f_{j_u} = 31.6 \text{ kHz}$ and $f_{j_w} = 3.05, 6.70, 12.44, 19.49, 28.1, 38.3 \text{ kHz}$ as verified by the $\text{imag}(FRF)$ plot. Note that the PWAS natural frequencies do not come into play here because the first PWAS resonance is way above the 40 kHz range (as indicated in Problem 9.2, the first PWAS frequency is around 300 kHz).

```

1 % Ch.10 Problems 10.3, 10.4, 10.5 (aluminum plates)
2 % Copyright Victor Giurgiutiu: SHM with PWAS book
3 clc
4 clear all
5 %% DEFINE PROPERTIES
6 a=100e-3/2; h=0.8e-3; E=70e9; nu=0.33; p=2700; % alum plate
7 D=E*h^3/12/(1-nu^2); % flexural stiffness of the plate
8 zetaU=10e-3; zetaW=10e-3; % structural damping
9 ra=7e-3/2; ta=0.2e-3; % PWAS geometry
10 sE11=15.30e-12; e0=8.85e-12; eT33=1750*e0; ...
11 d31=-175e-12;pa=7700; nua=0.35; % PWAS material
12 %% DEFINE FREQUENCY RANGE
13 kHz=1e3; % shorthand for kHz
14 Nf=401; % number of frequencies in the spectrum
15 fStart=1*kHz; % start frequency
16 fEnd=40*kHz; % end frequency
17 df=(fEnd-fStart)/(Nf-1); % frequency increment
18 f=fStart:df:fEnd; w=2*pi*f; % frequency range, f in Hz; w in rad/s
19 %% CALCULATE NATURAL FREQUENCIES AND MODESHAPES
20 Nr=1e3; dr=a/(Nr-1); r=0:dr:a; % discretize disc radius
21 %% define shorthand notations for Bessel functions
22 J0=@(z) besselj(0,z); J1=@(z) besselj(1,z); J2=@(z) besselj(2,z);
23 I0=@(z) besseli(0,z); I1=@(z) besseli(1,z); I2=@(z) besseli(2,z);
24 %% Axial frequencies and modeshapes:
25 % calculate axial eigenvalues: solve Eq. (10.57)
26 cL=sqrt(E/p/(1-nu^2));
27 funcU=@(z) (z*J0(z)/J1(z)-1); % characteristic eq-n for free-free axial vibr.
28 ffU=0; jU=0; NU_low=0; % starting values for the iteration loop
29 j=1:1:20; zUg=pi/2*(2*j-1); % initial guess for axial eigenvalues
30 while ffU<=fEnd % identify the required axial modes
31 jU=jU+1; % increment counter
32 z=fzero(funcU,zUg(jU)); % solve axial transcendal eq.
33 zU(jU)=z; % store axial eigenvalue
34 gU=z/a; % axial wave number
35 wU(jU)=cL*z/a; % store axial angular frequency in rad/s
36 fU(jU)=wU(jU)/(2*pi); % store axial frequency in Hz
37 AU=1/sqrt(J1(z)^2-J0(z)*J2(z)); % axial modeshape amplitude
38 U(:,jU)=AU*J1(gU*r); % axial modes
39 Ura(jU)=AU*J1(gU*ra); % axial displacement at PWAS edge r=ra
40 ffU=fU(jU); % local value of frequency for the interation loop
41 NU_low=NU_low+1*(ffU<fStart); % increment lower limit of mode index range
42 end
43
44 NU_low=1*(NU_low<1)+NU_low*(NU_low>=1); % lower limit on the axial modes index
45 NU_high=jU; % number of required axial modes
46 display(zU,'zU, kHz') % axial eigenvalues
47 display([jU,fU/kHz],'jU, fU, kHz') % axial frequencies
48 display([fStart/kHz fEnd/kHz],'fStart fEnd, kHz') % frequency range
49 display([NU_low, NU_high],'NU_low, NU_high') % axial mode index range
50
51 figure(1); plot(r,U);grid; title ('Axial modes')

```

```

52 %% Flexural frequencies and modeshapes
53 % calculate flexural eigenvalues: solve Eq. (10.65)
54 funcW=@(z) (z.*J0(z)-(1-nu).*J1(z))/(z.*I0(z)-(1-nu).*I1(z))+J1(z)/I1(z);
55 % characteristic equation for free-free flexural vibr.
56 ffW=0; jW=0; NW_low=0; % starting values for the iteration loop
57 j=1:1:20; zWg=pi*j; % initial guess for flexural eigenvalues
58 while ffW<=fEnd % identify the required flexural modes
59     jW=jW+1; % increment counter
60     z=fzero(funcW,zWg(jW)); % solve flexural transcendal eq.
61     zW(jW)=z; % store flexural eigenvalue
62     gW=z/a; % flexural wave number
63     wW(jW)=z^2*sqrt(D/p/h/a^4); % store flexural angular frequency in rad/s
64     fW(jW)=wW(jW)/(2*pi); % store flexural frequency in Hz
65     ffW=fW(jW); % local value of flexural frequency for the interation loop
66     NW_low=NW_low+1*(ffW<fStart); % increment lower limit of mode index range
67 % Calculate modeshapes: Eqs. (10.64)-(10.68)
68 C=-J1(z)/I1(z); % modeshape coefficient
69 InW=@(r) (J0(z*r/a)+C*I0(z*r/a)).^2.*r; % integrant for flex. ampl. calc.
70 IntW=integral(InW,0,a); % integral for flex. ampl. calc.
71 AW(jW)=a/sqrt(2)/sqrt(IntW); % flexural mode amplitude
72 % display([z C])
73 W(:,jW)=AW(jW)*(J0(z*r/a)+C*I0(z*r/a));
74 W1ra(jW)=AW(jW)*gW*(-J1(z*ra/a)+C*I1(z*ra/a)); % flexural slope at PWAS edge r=ra
75 end
76
77 NW_low=1*(NW_low<1)+NW_low*(NW_low>=1); % lower limit on the flex modes index
78 NW_high=jW; % upper limit on the flexural modes index
79 display(zW,'zW') % flexural roots
80 display(AW,'AW') % flexural amplitudes
81 display([jW,fW/kHz],'jW, fW, kHz') % flexural frequencies
82 display([fStart/kHz fEnd/kHz],'fStart fEnd, kHz') % frequency range
83 display([NW_low, NW_high],'NW_low, NW_high') % flexural mode index range
84
85 figure(2); plot(r,W); grid; title('Flexural modes')
86 % =====
87 %% START FREQUENCY LOOP TO CALCULATE FREQUENCY RESPONSE FUNCTIONS
88 ff=f/kHz; % freq in kHz for plotting
89 %% AXIAL RESPONSE
90 cU=2*ra/(p*h*a^2);
91 for nf=1:Nf % frequency loop
92     ww=w(nf);
93     % axial modes loop
94     sum_U=0;
95     for jU=NU_low:1:NU_high
96         etaU=1/(wU(jU)^2+2*1i*zetaU*wU(jU)*ww-ww^2);
97         sum_U=sum_U+cU*etaU*Ura(jU)^2;
98     end
99     FRF_U(nf)=sum_U;
100 end
101 %% PLOT AXIAL FRF
102 figure(3) % FRF_U plots

```

```

103 subplot(2,2,1); plot(ff,real(FRF_U));title('real FRF_U'); xlabel('f, kHz')
104 subplot(2,2,2); plot(ff,-imag(FRF_U));title('-imag FRF_U'); xlabel('f, kHz')
105 subplot(2,2,3); plot(ff,abs(FRF_U)); title('abs FRF_U'); xlabel('f, kHz')
106 %      set(gca,'Yscale','log');
107 subplot(2,2,4); plot(ff,180/pi*angle(FRF_U));...
108     title('angle FRF_U, deg'); xlabel('f, kHz')
109 %% FLEXURAL RESPONSE
110 cW=cU*(h/2)^2;
111 for nf=1:Nf % frequency loop
112     ww=w(nf);
113     % flexural modes loop
114     sum_Wl=0;
115     for jW=NW_low:1:NW_high
116 etaW=1/(wW(jW)^2+2*pi*zetaW*wW(jW)*ww-ww^2);
117     sum_Wl=sum_Wl+cW*etaW*Wlra(jW)^2;
118     end
119     FRF_W(nf)=sum_Wl;
120 end
121 %% PLOT FLEXURAL FRF
122 figure(4) % FRF_W plots
123 subplot(2,2,1); plot(ff,real(FRF_W));title('real FRF_W'); xlabel('f, kHz')
124 subplot(2,2,2); plot(ff,-imag(FRF_W));title('-imag FRF_W'); xlabel('f, kHz')
125 subplot(2,2,3); plot(ff,abs(FRF_W)); title('abs FRF_W'); xlabel('f, kHz')
126 %      set(gca,'Yscale','log');
127 subplot(2,2,4); plot(ff,180/pi*angle(FRF_W));...
128     title('angle FRF_W, deg'); xlabel('f, kHz')
129 %% COMBINE AXIAL AND FLEXURAL FRF
130 FRF=FRF_U+FRF_W; % Problem 10.3: combine axial and flex FRFs
131 % FRF=FRF_W; % Problem 10.4: flex FRF only (no axial)
132 % FRF=FRF_U; % Problem 10.5: axial FRF only (no flex)
133 %% PLOT COMBINED FRF
134 figure(5) % FRF plots
135 subplot(2,2,1); plot(ff,real(FRF));title('real FRF'); xlabel('f, kHz')
136 subplot(2,2,2); plot(ff,-imag(FRF));title('-imag FRF'); xlabel('f, kHz')
137 subplot(2,2,3); plot(ff,abs(FRF)); title('abs FRF'); xlabel('f, kHz')
138 %      set(gca,'Yscale','log');
139 subplot(2,2,4); plot(ff,180/pi*angle(FRF));...
140     title('angle FRF, deg'); xlabel('f, kHz')
141 %% STRUCTURAL STIFFNESS and STIFFNESS RATIO
142 kSTR_=1./FRF; % freq-dependent complex structural stiffness
143 figure(6) % kSTR plots
144 subplot(2,2,1); plot(ff,real(kSTR_));title('real kSTR'); xlabel('f, kHz')
145 subplot(2,2,2); plot(ff,imag(kSTR_));title('imag kSTR'); xlabel('f, kHz')
146 subplot(2,2,3); plot(ff,abs(kSTR_)); title('abs kSTR'); xlabel('f, kHz')
147 %      set(gca,'Yscale','log');
148 subplot(2,2,4); plot(ff,180/pi*angle(kSTR_));...
149     title('angle kSTR, deg'); xlabel('f, kHz')
150 figure(7) % superposed plot
151 plot(ff,real(kSTR_),ff,imag(kSTR_));
152     title('real kSTR, imag kSTR'); xlabel('f, kHz')
153 %% CALCULATE COMPLEX-NUMBER ELECTROMECHANICAL PWAS PROPERTIES

```

```

154 delta=1e-2; eta=1e-2; % PWAS mechanical damping and electrical loss factors
155 sE11_=(1-li*eta)*sE11; eT33_=(1-li*delta)*eT33; % complex PWAS mat. prop.
156 kp_2=2/(1-nua)*d31^2/sE11_/_eT33_; ...
157 % complex coupling coefficient in PWAS material
158 C_=eT33_*pi*a^2/ta; % complex capacitance of the PWAS
159 ca_=sqrt(1/pa/sE11_/(1-nua^2)); % complex axial wave speed in PWAS
160 kPWAS_=ta/a/sE11_/(1-nua); % complex stiffness of the PWAS
161 %% CALCULATE ADMITTANCE AND IMPEDANCE
162 chi_=kSTR_/kPWAS_; % freq-dependent complex stiffness ratio
163 phi_= w*a/2/ca_; % frequency dependent complex phi
164 num=(1+nua)*J1(phi_); % compose Eq.(10.85) using partial expressions
165 P1=(1-nua)-(1+nua)*chi_; den=phi_.*J0(phi_)-P1; A=num./den; P3=1-kp_2.*(1-A);
166 Y=li.*w.*C_.*P3; % admittance
167 Z=1./Y; % impedance
168 %% PLOT ADMITTANCE AND IMPEDANCE
169 figure(8) % Y plots
170 subplot(2,2,1); plot(ff,real(Y));title('real Y'); xlabel('f, kHz')
171 % set(gca,'Yscale','log');
172 subplot(2,2,2); plot(ff,imag(Y));title('imag Y'); xlabel('f, kHz')
173 subplot(2,2,3); plot(ff,abs(Y)); title('abs Y'); xlabel('f, kHz')
174 % set(gca,'Yscale','log');
175 subplot(2,2,4); plot(ff,180/pi*angle(Y));...
176 title('angle Y, deg'); xlabel('f, kHz')
177
178 figure(9) % Z plots
179 subplot(2,2,1); plot(ff,real(Z));title('real Z'); xlabel('f, kHz')
180 % set(gca,'Yscale','log');
181 subplot(2,2,2); plot(ff,imag(Z));title('imag Z'); xlabel('f, kHz')
182 subplot(2,2,3); plot(ff,abs(Z)); title('abs Z'); xlabel('f, kHz')
183 % set(gca,'Yscale','log');
184 subplot(2,2,4); plot(ff,180/pi*angle(Y));...
185 title('angle Z, deg'); xlabel('f, kHz')
186 %% SUPERPOSED PLOT OF Y, Z, FRF
187 maxY=max(abs(real(Y))); maxZ=max(abs(real(Z))); maxFRF=max(abs(imag(FRF)));
188 figure(10) % superposed plot of ReY, ReZ, -imagFRF
189 plot(ff,real(Y)/maxY,ff,real(Z)/maxZ,ff,-imag(FRF)/maxFRF);
190 title('real(Y), real(Z), -imag(FRF)'); xlabel('f, kHz')
191 % set(gca,'Yscale','log'); ylim([1e-3 2*1e0])
192
193
194
195
196
197
198
199

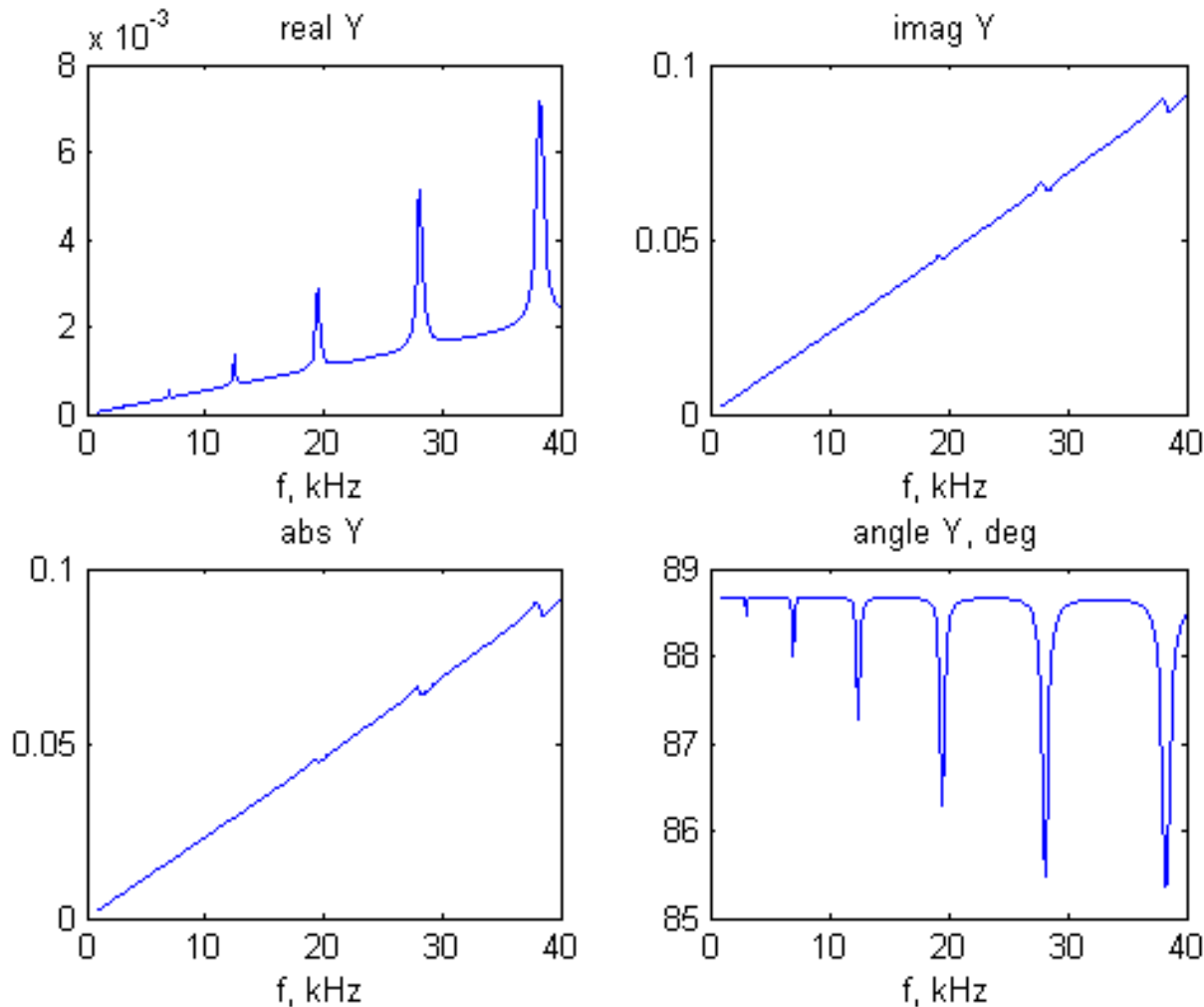
```

Problem 4: Repeat the calculations in Problem 3 above, but exclude the axial vibration from the structural stiffness calculation. Discuss your results

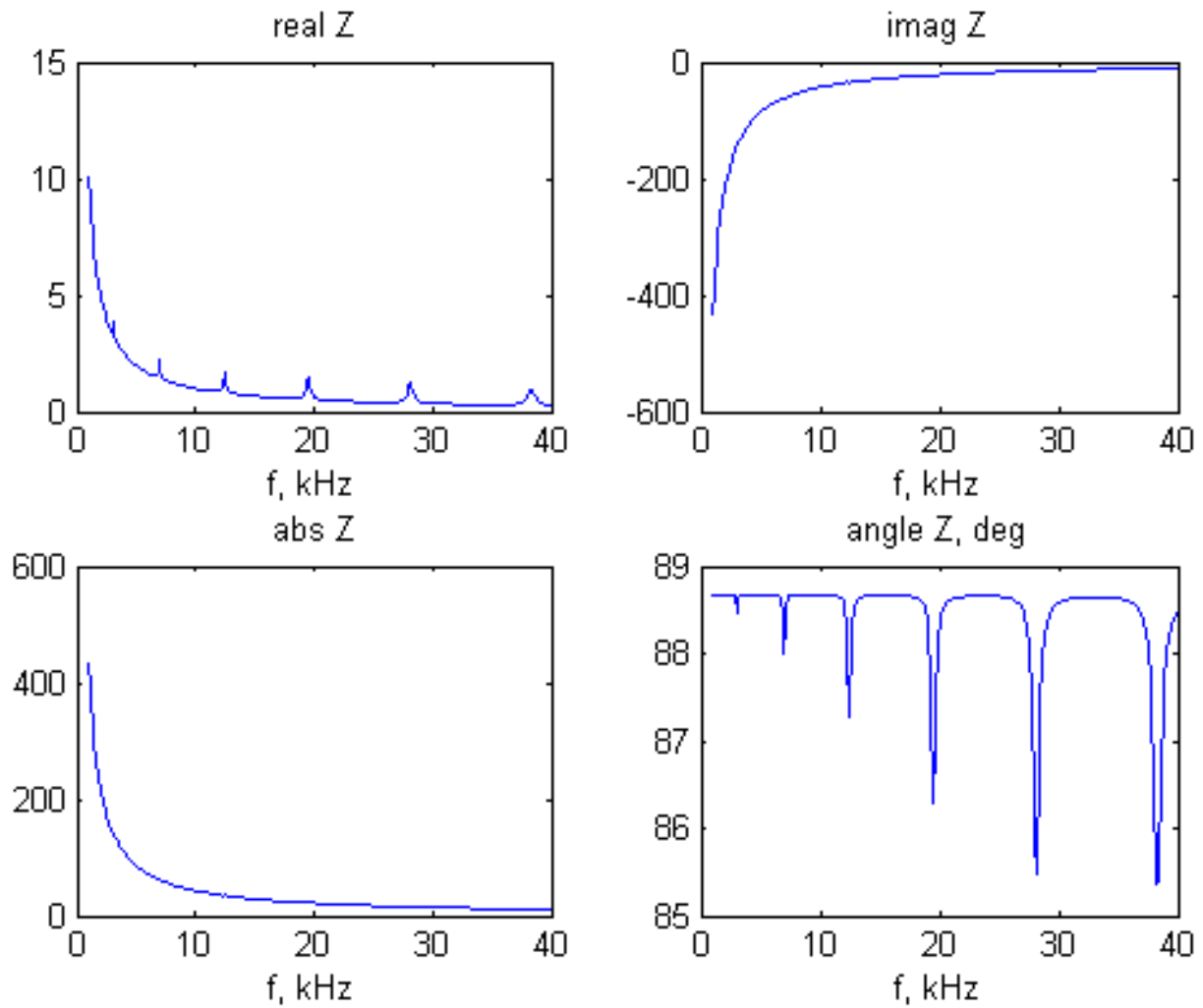
Solution

Repeating the calculations with the exclusion of axial vibration yields the following results:

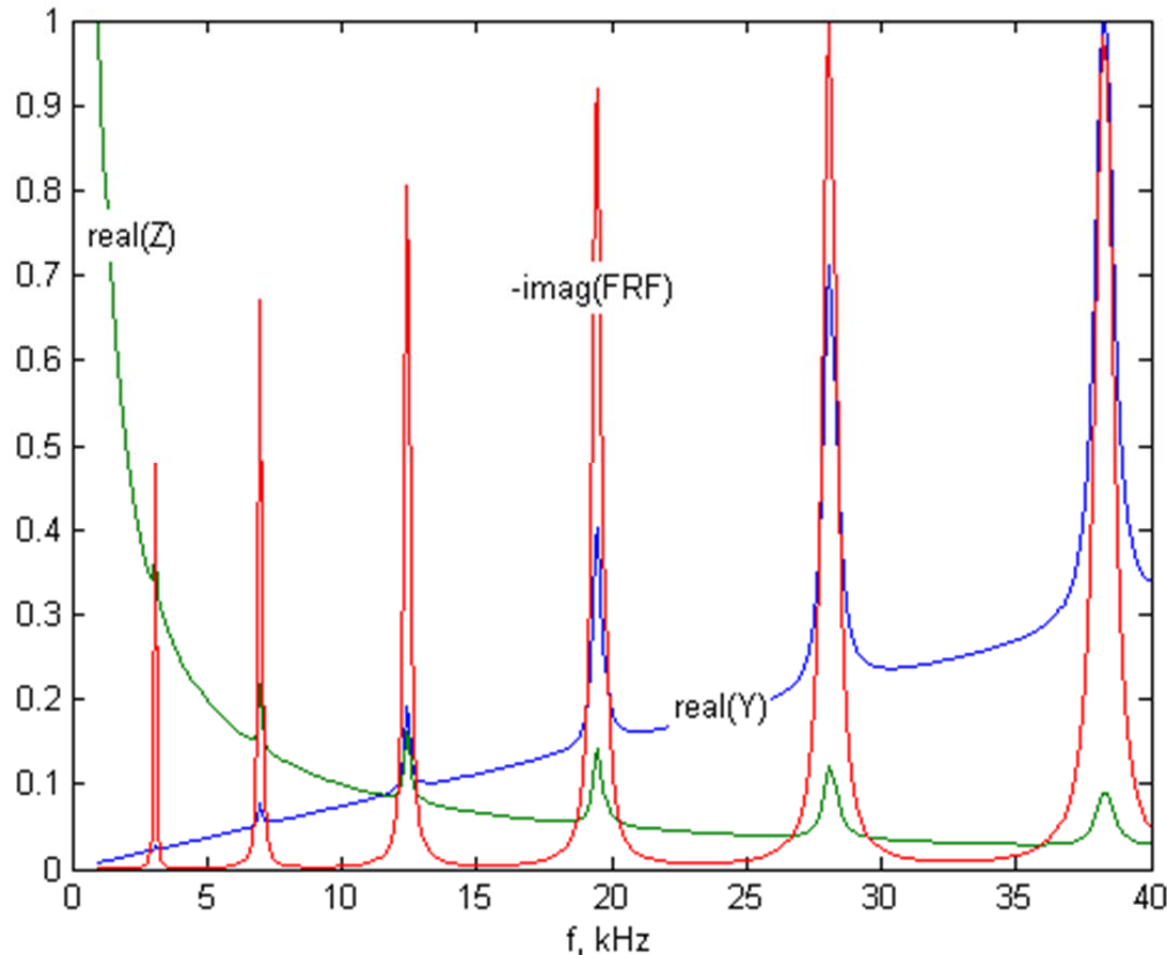
Admittance plot:



Impedance plot:



(ii) The superposed plot (with appropriate scale factors) of the admittance real part, $\text{real}(Y)$, impedance real part, $\text{real}(Z)$, and frequency response function imaginary part, $-\text{imag}(FRF)$ is shown below.



Comment: The peaks observed in these plots correspond to the natural frequencies of flexural vibration of the circular plate $f_{j_w} = 3.05, 6.70, 12.44, 19.49, 28.1, 38.3$ kHz as verified by the $\text{imag}(FRF)$ plot. Note that the PWAS natural frequencies do not come into play here because the first PWAS resonance is way above the 40 kHz range (as indicated in Problem 9.2, the first PWAS frequency is around 300 kHz).

Discussion: the exclusion of axial vibration from the analysis has reduced the number of resonance peaks from eight to seven. We notice that the peak at 35.86 kHz no longer appears in the analysis. Otherwise, the general shape of the admittance, impedance, and FRF functions is preserved.

```

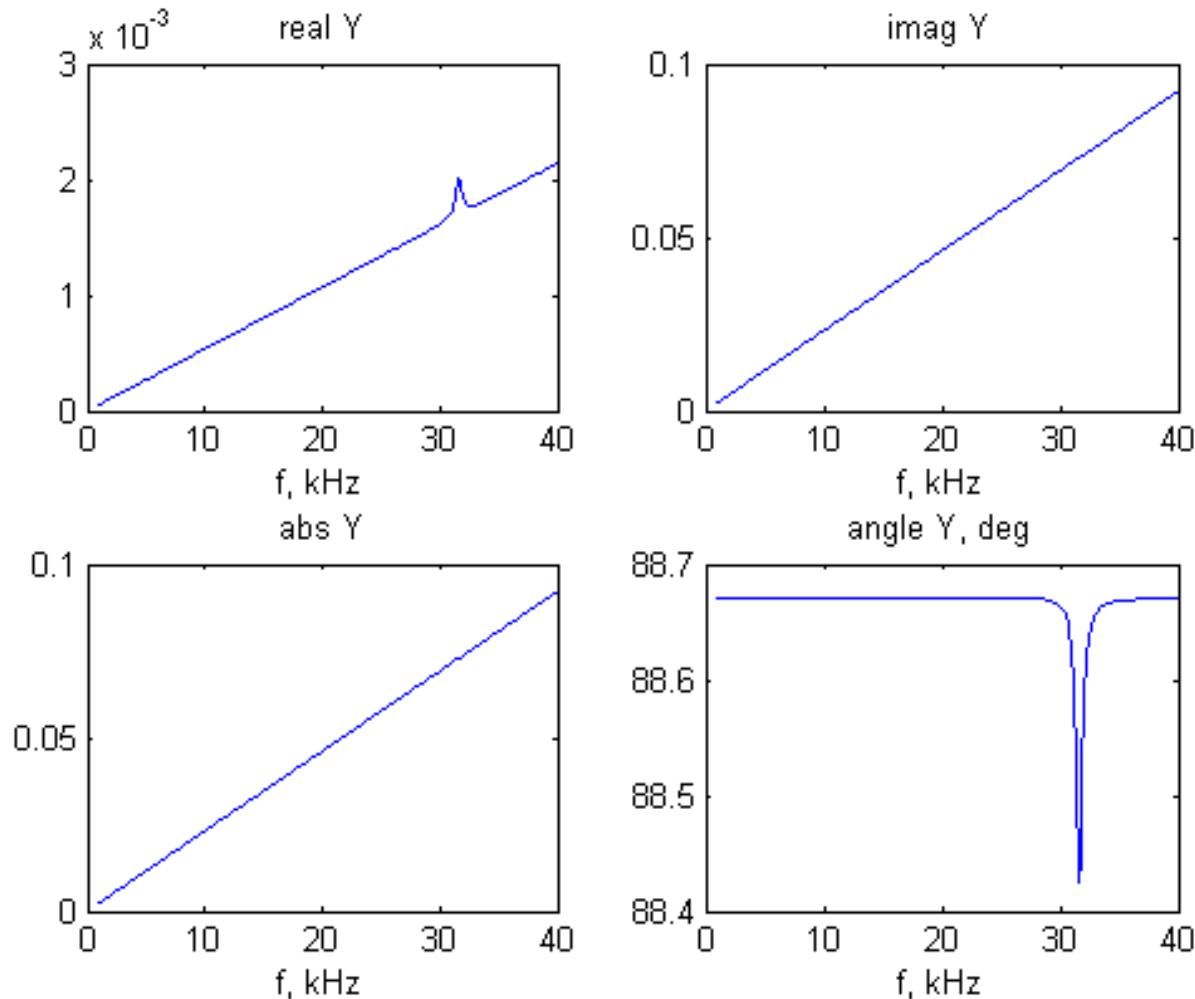
1 + % Ch.10 Problems 10.3, 10.4, 10.5 (aluminum plates)
5 + % DEFINE PROPERTIES
12 + % DEFINE FREQUENCY RANGE
19 + % CALCULATE NATURAL FREQUENCIES AND MODESHAPES
21 + % define shorthand notations for Bessel functions
24 + % Axial frequencies and modeshapes:
51 + % Flexural frequencies and modeshapes
84 + % START FREQUENCY LOOP TO CALCULATE FREQUENCY RESPONSE FUNCTIONS
86 + % AXIAL RESPONSE
98 + % PLOT AXIAL FRF
106 + % FLEXURAL RESPONSE
118 + % PLOT FLEXURAL FRF
126 - % COMBINE AXIAL AND FLEXURAL FRF
127 % FRF=FRF_U+FRF_W; % Problem 10.3: combine axial and flex FRFs
128 - FRF=FRF_W; % Problem 10.4: flex FRF only (no axial)
129 - % FRF=FRF_U; % Problem 10.5: axial FRF only (no flex)
130 + % PLOT COMBINED FRF
138 + % STRUCTURAL STIFFNESS and STIFFNESS RATIO
150 + % CALCULATE COMPLEX-NUMBER ELECTROMECHANICAL PWAS PROPERTIES
158 + % CALCULATE ADMITTANCE AND IMPEDANCE
165 + % PLOT ADMITTANCE AND IMPEDANCE
183 + % SUPERPOSED PLOT OF Y, Z, FRF
190
191
192
193
194
195

```

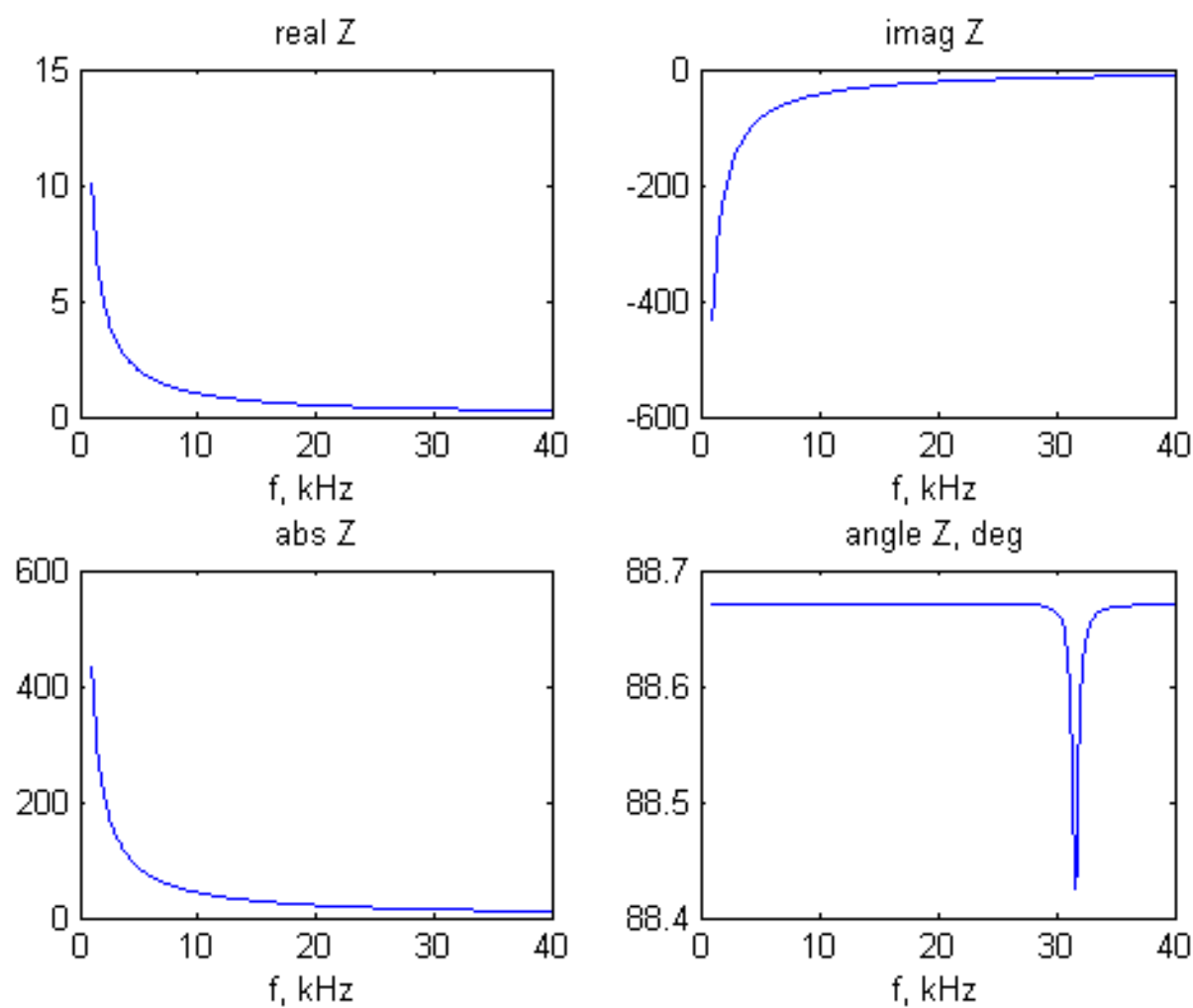
Problem 5: Repeat the calculations in Problem 3 above, but exclude the flexural vibration from the structural stiffness calculation. Discuss your results

Solution

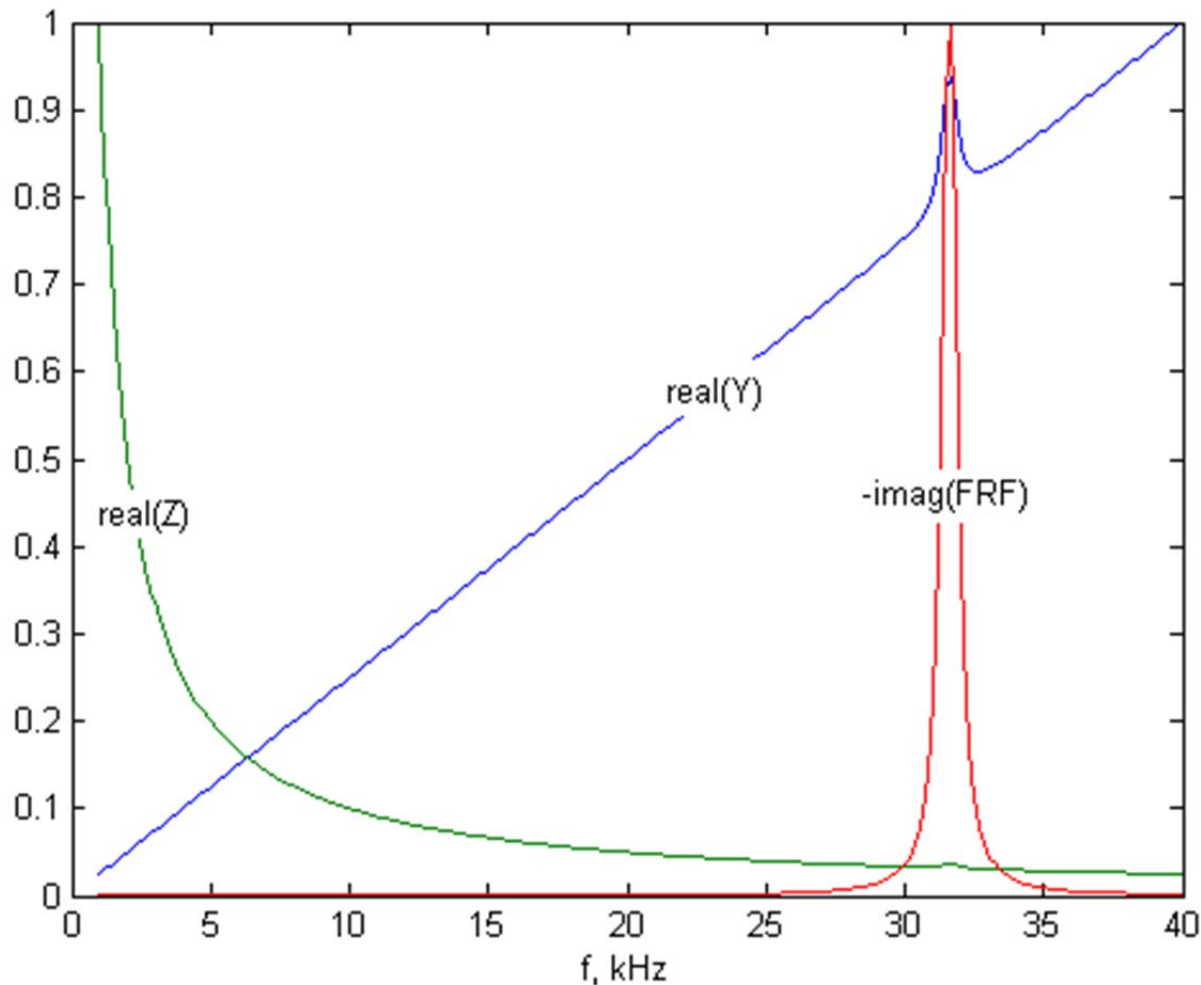
Repeating the calculations with the exclusion of axial vibration yields the following results:
Admittance plot:



Impedance plot:



(ii) The superposed plot (with appropriate scale factors) of the admittance real part, $\text{real}(Y)$, impedance real part, $\text{real}(Z)$, and frequency response function imaginary part, $-\text{imag}(FRF)$ is shown below.



Comment: The peaks observed in these plots correspond to the natural frequencies of axial vibration of the circular plate $f_{j_u} = 31.6$ kHz as verified by the $\text{imag}(FRF)$ plot. Note that the PWAS natural frequencies do not come into play here because the first PWAS resonance is way above the 40 kHz range (as indicated in Problem 9.2, the first PWAS frequency is around 300 kHz).

Discussion: the exclusion of flexural vibration has greatly simplified the analysis, since in the frequency range of interest (1-40 kHz) there is only one axial vibration resonance at 35.86 kHz. Hence, all the charts for this problem show only one resonance peak, located at this frequency. The last chart, containing admittance real part, impedance real part, and FRF imaginary part, is quite eloquent: it shows clearly and unequivocally that the resonance frequency can be very clearly identified with the peaks of these functions.

```

1 % Ch.10 Problems 10.3, 10.4, 10.5 (aluminum plates) % % %
5 % % % % %
12 % % % % %
19 % % % % %
21 % % % % %
24 % % % % %
51 % % % % %
84 % % % % %
86 % % % % %
98 % % % % %
106 % % % % %
118 % % % % %
126 % % % % %
127 % FRF=FRF_U+FRF_W; % Problem 10.3: combine axial and flex FRFs
128 % FRF=FRF_W; % Problem 10.4: flex FRF only (no axial)
129 - FRF=FRF_U; % Problem 10.5: axial FRF only (no flex)
130 % % % % %
138 % % % % %
150 % % % % %
158 % % % % %
165 % % % % %
183 % % % % %
190 % % % % %
191 % % % % %

```